THE IMPACT OF ACTIVE AERODYNAMICS ON MOTORCYCLES USING COMPUTATIONAL FLUID DYNAMICS SIMULATIONS

By,
Venkata Aditya Sripathi

A Thesis submitted in partial fulfillment of the requirements for the
Master of Science Degree
In
Automotive Engineering Technology
Minnesota State University, Mankato
May 2017

www.manaraa.com

ProQuest Number: 10282520

All rights reserved

INFORMATION TO ALL USERS
The quality of this reproduction is dependent upon the quality of the copy submitted.

In the unlikely event that the author did not send a complete manuscript
and there are missing pages, these will be noted. Also, if material had to be removed,
a note will indicate the deletion.

ProQuest 10282520

Published by ProQuest LLC (2017). Copyright of the Dissertation is held by the Author.

All rights reserved.
This work is protected against unauthorized copying under Title 17, United States Code
Microform Edition © ProQuest LLC.

ProQuest LLC.
789 East Eisenhower Parkway
P.O. Box 1346
Ann Arbor, MI 48106 – 1346

www.manaraa.com

05/10/2017

The Impact of Active Aerodynamics on Motorcycles Using Computational Fluid Dynamics Simulations

Venkata Aditya, Sripathi

This thesis has been examined and approved by the following members of the student's committee.

_____

Dr. Craig T. Evers – Committee Chair and Advisor

_____

Dr. Kuldeep Agarwal – Committee Member

_____

Dr. Winston Sealy – Committee Member

www.manaraa.com

ACKNOWLEDGEMENTS

Motorcycling is a beautiful world. I will forever be indebted to everyone who has been aside me in this world of happiness. I dedicate this project to my parents, Subbarao Sripathi & Rajeshwari Sripathi and my brother, Venkata Akshay Sripathi who have been with me through every phase of my life and have only helped me move in the right direction always. My friend Shamkumar Mahurkar deserves a special acknowledgment as he has been responsible for teaching me CFD as a subject and continuously helping me with my project as a co-author. I would like to thank my friends and extended family members who have always kept me motivated and dedicated to the world of motorcycling and traveling. I would like to thank my professors from Minnesota State University, Mankato for helping me reach this stage where I am able to demonstrate academic and scientific excellence. My special thanks go to Dr. Craig Evers, Dr. Kuldeep Agarwal, Dr. Winston Sealy, Dr. Bruce Jones, Dr. Ahmed Shaheen and Mr. Kevin Schull for taking a keen interest in my academic research and always guiding me onto the right path. I would also like to deeply thank Ms. Chelsea Skluzacek who has been my mentor and my direct supervisor at the Alumni & Foundation Center for instilling the work ethics and positivity in me. I would like to thank ANSYS Inc. and PTC for their software package which has immensely helped me in conducting research at an academic level. I would also like to especially thank Microsoft Corporation for the Operating system and their Office Suite without which this thesis would have never been possible. I would like to extend my gratitude towards the Automotive Engineering Department and the Mechanical Engineering Department at the University for allowing research to be conducted utilizing their resources. Lastly, huge thanks to everyone who has been a part of this journey so far and to the world of good where I believe everyone has the chance to make a difference.

www.manaraa.com

ABSTRACT

Title of Thesis: The Impact of Active Aerodynamics on Motorcycles Using Computational Fluid Dynamics

Degree Candidate: Venkata Aditya, Sripathi

Degree: Master of Science in Automotive Engineering 2017

Minnesota State University, Mankato, MN

Motorcycles are mostly utilized by commuters whose requirements are cheap and affordable transportation from point A to point B. Motorcycles also provide means to tour various places and have a leisure time for the majority of motorcyclists. Unfortunately, with pros also come cons such as accidents which are disabling or life-taking. According to motorcycle crash statistics produced every year, the majority of motorcycle crashes are caused due to facing unexpected obstacles in the path causing collisions due to insufficient braking time. Thus, this thesis serves as a mean to overcome this issue and provide a technological solution to the world of motorcyclists.

The thesis initially covers the introduction to the history of Computational Fluid Dynamics and Simulations. Consequently, the modeling aspects of the motorcycle and the active aerodynamics concepts are studied and explained in detail in conjunction with the usage of PTC Creo 3.0. The subsequent chapters explain the Computational Fluid Dynamics simulations setup, processing and post processing of the results utilizing ANSYS Workbench and its modules Design Modeller, Mesh, FLUENT and Post Process. Finally, the rapid prototyping using Stratasys UPrint 3D Printing and wind tunnel validation aspects of the project are discussed leading to key conclusions and discussions.

This thesis is aimed to be an innovation to help protect motorcyclists from fatalities and also stands as a means to demonstrate engineering capabilities in producing real-world solutions through low-cost and viable simulation sciences.

Keywords: Motorcycles, Motorcycle Safety, Computational Fluid Dynamics, Aerodynamic Braking, Active Aerodynamics, Modelling and Simulations, Computer Aided Design, Computer Aided Engineering, ANSYS, FLUENT, PTC Creo, External Flow Analysis and Testing, Wind Tunnel Testing, Rapid Prototyping, Additive Manufacturing, 3D Printing.

www.manaraa.com

TABLE OF CONTENTS

ACKNOWLEDGEMENTS ii
ABSTRACT iii
TABLE OF CONTENTS iv
LIST OF FIGURES vi
LIST OF TABLES viii
NOMENCLATURE ix
ACRONYMS ix
CONSTANT VALUES ix
CHAPTER 1 – LITERATURE REVIEW 1
CHAPTER 2 – INTRODUCTION 2
INTRODUCTION TO FLUIDS 2
INTRODUCTION TO FLUID DYNAMICS 2
INTRODUCTION TO COMPUTATIONAL FLUID DYNAMICS 2
FINITE VOLUME METHOD 3
UNDERLYING LAWS 4
K–ω MODEL 10
GAMMA–RETHETA MODEL 10
LANGTRY–MENTER 4–EQUATION TRANSITIONAL SST MODEL 11
COMPUTATIONAL FLUID DYNAMICS – MODELING 12
COMPUTATIONAL FLUID DYNAMICS – MESHING 13
COMPUTATIONAL FLUID DYNAMICS – SIMULATION SETUP 14
COMPUTATIONAL FLUID DYNAMICS – POST PROCESSING 14
CHAPTER 3 – DESIGN AND MODELING 15
THE DESIGN PROCESS 15
THE MOTORCYCLE 15
THE AIRFOILS 18
THE MOTORCYCLE-AIRFOIL ASSEMBLIES 19
THE WIND TUNNEL 19
CHAPTER 4 – COMPUTATIONAL RESEARCH 20
PRE-PROCESSING 20
SIMULATION SETUP 21
ANALYSIS OF COMPUTATIONAL RESULTS 22
POST PROCESSING AND VISUALIZATIONS 23
CHAPTER 5 – PRODUCTION PROCESS 24
CHAPTER 6 – WIND TUNNEL TESTING 25

www.manaraa.com

QUANTITATIVE TESTING 25
QUALITATIVE TESTING 26
CHAPTER 7 – ANALYSES AND RESULTS 27
QUANTITATIVE STUDY 27
QUALITATIVE STUDY 28
CHAPTER 8 – CONCLUSIONS AND FUTURE SCOPE 30
RESULTS AND CONCLUSIONS 30
FUTURE SCOPE AND RECOMMENDATIONS 31
APPENDIX 32
WIND TUNNEL APPARATUS SETUP 32
ELD WIND TUNNEL ELECTRONIC DISPLAY MACHINE OUTPUT 34
BIBLIOGRAPHY 41

www.manaraa.com

LIST OF FIGURES

Figure 1. Comparison between Traditional vs. CFD Techniques (Maria, 1997, p. 8). 3
Figure 2. Fluid particle Fixed in space vs. a Dynamic Fluid Particle (J.D. Anderson, 2009, pp. 17, 19) 4
Figure 3. Infinitesimal element flowing through a 3D space (J.D. Anderson, 2009, p. 28). 8
Figure 4. Comparison between a Mathematical (CAD) Model and a Physical Model. 12
Figure 5. Importance of Meshing (Nitin & Lee, 2008). 13
Figure 6. Demonstration of a 3D Mesh. Courtesy: Tata Johnson Controls Automotive Limited, India. 13
Figure 7. Snapshots of Post Processing Results Using Streamline and Contour Plots (T.M.V Engineering Blog, n.d.). 14
Figure 8. Pictures of the Side and the Front View of a 2005 Honda CBR1000RR Fireblade (MCN Bikes For Sale, n.d.). 15
Figure 9. Snapshot of the PTC Creo V 3.0 User 3D Space with Reference Images in Planes. 16
Figure 10. LEFT – Fairing Sketch-Up. RIGHT - Engine Area Sketch-Up using the Extruded Fairing as Reference. 16
Figure 11. Sketch-Up (Using Side View) ➔ Extrude ➔ Carve (Using Front View) Design Process in Pictures. 17
Figure 12. Refinements - Headlamps, Rounded Fairing Edges, Front-End Modified, and Tail-End Straightened. 17
Figure 13. NACA 6412 IL Airfoil Profile (UIUC Airfoil Coordinates Database, n.d.). 18
Figure 14. The difference between Lift and Downforce produced by an Airfoil. 18
Figure 15. LEFT TO RIGHT - Non-Wing, 0 Degrees, 10 Degrees and 90 Degrees CAD models. 19
Figure 16. Virtual Wind Tunnel CAD Model with Motorcycle CAD Model. 19
Figure 17. LEFT: C Type Hyperbolic Grid Mesh (Thisse, 2004). RIGHT: Polyhedral Mesh (Park, Hong, Kim, & Lee, 2008). 20
Figure 18. 3D Unstructured Grid Mesh with Sizing of 5mm at the Motorcycle Body (Region of Interest). 21
Figure 19. FROM TOP LEFT CLOCKWISE: Streamline Plot, Velocity Contour, Pressure Contour and Vector Plot. 23
Figure 20. Finalized 3D Printed Models. FROM LEFT: Non-Wing, 0 Degrees, 10 Degrees and 90 Degrees Models. 24
Figure 21. Visualization Testing using the Wind Tunnel. LEFT: Headlamp area showing the flow separation, the stagnation point and vortices behind the windblast area. RIGHT: Tail end vortices a.k.a. Wake of the Motorcycle. 26

www.manaraa.com

Figure 22. Validation of CFD Results: Stagnation Point at the Front, Vortices behind Windshield. 28
Figure 23. Validation of CFD Results: Vortices Formation under Tail Section and Streamlines behind the Wheel. 28
Figure 24. Validation of CFD Results: Wingtip Vortices and Flow Deflection due to the Airfoil. 29
Figure 25. Validation of CFD Results: Vortex Core Region Formation. 29
Figure 26. Graphical Representation of Lift vs. Dragforce figures. 31
Figure 27. The Strut, Mounting Fixture in the Wind Tunnel. 32
Figure 28. SAI Bubble Solution Equipment, Strut, Mounting Fixture, Prototype and Pitot Tube Assembly. 33
Figure 29. Non-Wing Prototype Gauge Indication at Zero Wind Speed. 34
Figure 30. Non-Wing Prototype Gauge Indication at 44.7m/s i.e. Test Wind Speed. 35
Figure 31. 0 Degree Wing Prototype Gauge Indication at Zero Wind Speed. 36
Figure 32. 10 Degree Wing Prototype Gauge Indication at Zero Wind Speed. 37
Figure 33. 10 Degree Wing Prototype Gauge Indication at 44.7m/s i.e. Test Wind Speed. 38
Figure 34. 90 Degree Wing Prototype Gauge Indication at Zero Wind Speed. 39
Figure 35. 90 Degree Wing Prototype Gauge Indication at 44.7m/s i.e. Test Wind Speed. 40

www.manaraa.com

LIST OF TABLES

Table 1. Simulation Setup Parameters in ANSYS Fluent for the Thesis.....22
Table 2. Table of Coefficients of Lift and Drag obtained from ANSYS Fluent. 22
Table 3. Lift and Drag Forces on all models obtained through CFD Testing.....23
Table 4. Lift and Drag Forces on all models obtained through Wind Tunnel Testing. 26
Table 5. Comparison of Results between CFD and Wind Tunnel Forces Data.....27
Table 6. Improvements in Downforce - Non-Wing vs. 0 Degree Wing Model.....30
Table 7. Improvements in Downforce - Non-Wing vs. 10 Degree Wing Model.....30
Table 8. Improvements in Drag Force - Non-Wing vs. 90 Degree Wing Model.....30

www.manaraa.com

NOMENCLATURE

C_L	–	Coefficient of Lift
C_D	–	Coefficient of Drag
ρ	–	Density of Air
V	–	Wind Speed (in m/s)
A_L	–	Lifting Area of the body
A_D	–	Frontal (Drag) Area of the body
F_L	–	Lift Force acting on the body $= \frac{1}{2}\rho A V^2 C_L$
F_D	–	Drag Force acting on the body $= \frac{1}{2}\rho A V^2 C_D$
α	–	Attack Angle in degrees
s	–	Displacement
T	–	Temperature
τ	–	Shear Stress
ω	–	Specific turbulence dissipation rate
$\widetilde{Re}_{\theta t}$	–	Local transition onset momentum thickness Reynolds number
k	–	Turbulence Kinetic Energy
θ	–	Momentum thickness

ACRONYMS

CFD	–	Computational Fluid Dynamics
CAD	–	Computer Aided Design

CONSTANT VALUES

To avoid any misconceptions due to different definition-styles across various literatures, the following values yield throughout this document. They are mainly based on the standard values provided by ANSYS Fluent.

g_0	=	9.81 $[ms^{-2}]$
ρ_∞	=	1.225 $[Kg/m^3]$
T_∞	=	288.16 $[K]$

www.manaraa.com

CHAPTER 1 – LITERATURE REVIEW

The field of Computational Sciences has significantly advanced over the past few decades. It includes a wide array of areas such as Computational Fluid Dynamics and Computer Aided Engineering. It is used in many fields such as evaluating air flows, fluid flows, predicting crash simulations, fatigue analyses, and explicit dynamics. Computational Sciences are used across a multitude of industries ranging from Engineering to National Defence. The utilization of the Modelling & Simulation techniques in the field of Medical Sciences is an emerging trend in the current industry as well.

This thesis deals with the application of Computational Fluid Dynamics techniques to obtain a real-world engineering solution for motorcycling applications. Fluid Dynamics is the science of fluid flows and their various properties. "The cornerstone of computational fluid dynamics is the fundamental governing equations of fluid dynamics—the continuity, momentum, and energy equations." (J.D. Anderson, 2009). In simpler terms, these refer to the conservation of mass, conservation of momentum and conservation of energy. The entirety of CFD is based on these fundamental equations.

The study aims to shed light on the three fundamentals of CFD and their impact on the various approaches used over the course of the thesis experimentation. The initial section illustrates the modeling aspects of the Motorcycle body and the aerodynamic structures using CAD techniques. This is followed by insights into the CFD modeling of the various test concepts explained over the course of this paper. The CFD section includes the modeling of the test environment, meshing the domains and setting up the simulations. A separate section is dedicated to analyzing the results of the post-processing tools.

Validation of the CFD results is performed through Wind-Tunnel testing. The models required for the wind tunnel testing are manufactured through additive manufacturing, the aspects of which are discussed in the subsequent section of the report. Various test concepts are shown and the key aspects of additive manufacturing are highlighted. The next section focuses on the wind tunnel testing and its various aspects. The key points include obtaining force reports on the motorcycle and producing illustrations of streamline flows across the motorcycle body in correlation to the CFD results.

The conclusions are drawn eventually from all the studies performed and results are obtained. This section focuses on inferences drawn from the study and providing a simpler conclusion, appealing to a wider audience. The limits and exclusions along with aspects for further research are discussed in the final chapter of this paper.

The basis for this research has been possible due to the prior studies performed by other researchers. The two significant researches done by (Sedlak, 2012) and (Goudar & Lalwani, 2014) are the primary resources for this research to be possible. The combination of the ideas presented by those researches is the key idea behind this thesis.

www.manaraa.com

CHAPTER 2 – INTRODUCTION

INTRODUCTION TO FLUIDS

The term fluid refers to any substance that can flow or continually deform under an applied shear stress (Edinformatics - What are Fluids?, n.d.)[1]. Few of the most common fluids we utilize frequently include water, oils and also the air we breathe in. There are three types of matter predominantly; solids, liquids, and gases. Fluids are characterized by moderately strong intermolecular forces, their ability to deform and compress to a very high degree and their property of being shapeless. Both fluids and gases are collectively considered as fluids as their behavior under applied forces is similar.

INTRODUCTION TO FLUID DYNAMICS

Fluid dynamics deals with how fluids behave under various circumstances and their properties. Fluid dynamics is the study of fluid flow, convective heat transfer, and species mass transfer[2].These fundamentals can be applied to various real-world cases to predict air flows and fluid flows in various fluid systems. The earliest example of fluid mechanics was demonstrated by Archimedes, a Greek physicist, mathematician, and philosopher. His experiments to evaluate the authenticity of King Hiero II's gold crown led him to a discovery that is now termed as Buoyancy. His principle, called as the Archimedes' Principle states that the amount of fluid displaced by a body or the buoyant force exerted by the fluid is equal to the weight of the solid. His discovery led to the inception of the field of Hydrostatics. Presently, buoyancy is a discovery that is used in the design of ships, hot air balloons, and blimps. The field of fluid mechanics & dynamics has expanded over the years into industries such as aerospace, automotive, geoscience and health care.

INTRODUCTION TO COMPUTATIONAL FLUID DYNAMICS

Computational Fluid Dynamics or CFD for short is the modern day incarnation of the field of fluid dynamics. Computational Fluid Dynamics (CFD) is the method of applying the governing equations of fluid dynamics and advancing these equations in space and/or time to obtain an approximate solution to a fluid dynamics and heat transfer practical application (Zikanov, 2010, p. 1). As the term is coined, the literal meaning of CFD is fluid dynamics studied in a computer/computational environment. The key behind this is to utilize the computational power of modern-day computer processors to validate the concepts of fluid dynamics. Computer Simulations are used to verify and produce results of real-world situations. A comparison between the traditional methods and CFD techniques by (Maria, 1997) can be used for a clearer understanding as illustrated below.

[1] *What are fluids?* Retrieved from http://www.edinformatics.com/math_science/what_are_fluids.htm

[2] *Air Flow and Rain Water Penetration Analysis on Generator Enclosures Using CFD Simulations – Sasanka K Andawatta* Retrieved from http://cornerstone.lib.mnsu.edu/etds/434/

www.manaraa.com

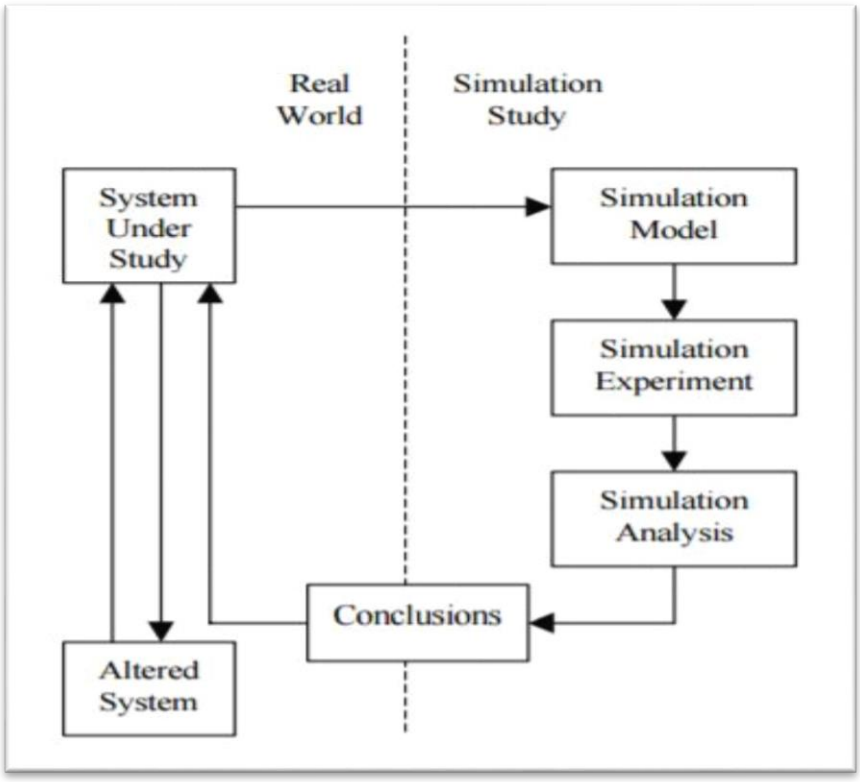

Figure 1. Comparison between Traditional vs. CFD Techniques (Maria, 1997, p. 8).

As we can see, the traditional approach includes constant back and forth between design and testing. The modern approach to a problem involves modeling the concept and carrying out computerized simulations to achieve results in an approximation to the traditional methods. Currently, the science of modeling & simulations is regarded as a National Critical Technology (National Training and Simulation Association , 2011). The various aspects of the simulation processes involved in a CFD study are described in the next sections of this chapter.

FINITE VOLUME METHOD

Discretization is a key element of computational fluid dynamics. Discretization is the method of approximating the differential equations by a system of algebraic equations for the variables at some set of discrete locations in space and time (J.H.Ferziger, 2002). There are many approaches but the most popular ones include Finite Difference (FD), Finite Element (FE) and Finite Volume (FV).

The finite volume method uses the integral form of the conservation equations as its starting point. The solution domain is divided into a large number of control volumes (CVs) and the conservation equations are applied to each CV. Interpolation is applied to express variables at the surface in terms of the values obtained by calculating the variable values at the computational node of each CV. The Finite Volume method is popular as it can accommodate any type of a grid and is suitable for complex geometries.

www.manaraa.com

UNDERLYING LAWS

The underlying laws of fluid dynamics are conservation of mass and conservation of momentum. These equations are coupled across various flow conditions and effectively produce the resultant flows of fluids such as air. A brief introduction is provided onto these principles and their governing equations as follows.

THE SUBSTANTIAL DERIVATIVE

An infinitesimal fluid particle is considered for an explanation. As (J.D. Anderson, 2009) stated, "The fluid element is infinitesimal in the same sense as differential calculus; however, it is large enough to contain a huge number of molecules so that it can be viewed as a continuous medium. Thus, instead of looking at the whole flow field at once, the fundamental physical principles are applied to just the fluid element itself. This application leads directly to the fundamental equations in partial differential equation form." The fluid particle can be considered fixed in space or can be visualized as a dynamic particle whose properties change with respect to time as shown in Figure 2.

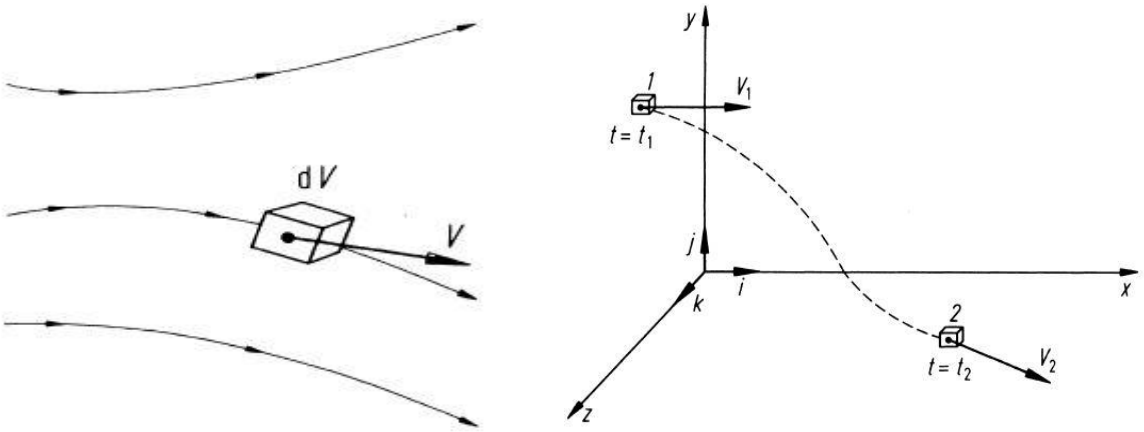

Figure 2. Fluid particle Fixed in space vs. a Dynamic Fluid Particle (J.D. Anderson, 2009, pp. 17, 19).

In the case of the study being performed in this thesis, the flow being dealt with is a dynamic flow, meaning the fluid particles are in motion constantly from point A to point B. This motion is performed between time intervals and the properties such as density physically change with respect to the particle's motion along the 3D spatial coordinates x, y, and z.

The vector equation representing the velocity field is as follows,

$$\vec{V} = u\vec{\imath} + v\vec{j} + \overrightarrow{wk}$$

Equation 1

www.manaraa.com

Where in the x, y and z components of the velocity are given by,

$$\boldsymbol{u = u(x, y, z, t)}$$

Equation 2

$$\boldsymbol{v = v(x, y, z, t)}$$

Equation 3

$$\boldsymbol{w = w(x, y, z, t)}$$

Equation 4

Initially, the particle is at point 1. The density and time of the particle are as follows,

$$\boldsymbol{\rho_1 = \rho(x_1, y_1, z_1, t_1)}$$

Equation 5

At the end of its dynamic motion, the particle is at point 2. The density and time are,

$$\boldsymbol{\rho_2 = \rho(x_2, y_2, z_2, t_2)}$$

Equation 6

These functions can be expanded into the form of a Taylor Series as follows,

$$\boldsymbol{\rho_2 = \rho_1 + \left\{\left(\frac{\partial \rho}{\partial x}\right)_1 (x_2 - x_1)\right\} + \left\{\left(\frac{\partial \rho}{\partial y}\right)_1 (y_2 - y_1)\right\} + \left\{\left(\frac{\partial \rho}{\partial z}\right)_1 (z_2 - z_1)\right\} + \left\{\left(\frac{\partial \rho}{\partial t}\right)_1 (t_2 - t_1)\right\} + \{Higher\ Order\ Terms\}}$$

Equation 7

By not including the higher order terms and diving Equation 7 by $(t_2 - t_1)$, we get,

$$\boldsymbol{\left(\frac{\rho_2 - \rho_1}{t_2 - t_1}\right) = \left\{\left(\frac{\partial \rho}{\partial x}\right)_1 \left(\frac{x_2 - x_1}{t_2 - t_1}\right)\right\} + \left\{\left(\frac{\partial \rho}{\partial y}\right)_1 \left(\frac{y_2 - y_1}{t_2 - t_1}\right)\right\} + \left\{\left(\frac{\partial \rho}{\partial z}\right)_1 \left(\frac{z_2 - z_1}{t_2 - t_1}\right)\right\} + \left\{\left(\frac{\partial \rho}{\partial t}\right)_1\right\}}$$

Equation 8

The left-hand side of Equation 8 is the average change of density over the change of time from t_2 to t_1. By limitation of the time from $t_2 \rightarrow t_1$, we get the instantaneous time rate change of density given by the right hand sided term of Equation 5 as follows,

$$\boldsymbol{\lim_{t_2 \rightarrow t_1} \left(\frac{\rho_2 - \rho_1}{t_2 - t_1}\right) = \frac{D\rho}{Dt}}$$

Equation 9

www.manaraa.com

Also, the instantaneous time rates of change over x, y and z can be notated as follows,

$$\lim_{t_2 \to t_1} \left(\frac{x_2 - \rho_1}{t_2 - t_1} \right) = u$$

Equation 10

$$\lim_{t_2 \to t_1} \left(\frac{\rho_2 - \rho_1}{t_2 - t_1} \right) = v$$

Equation 11

$$\lim_{t_2 \to t_1} \left(\frac{\rho_2 - \rho_1}{t_2 - t_1} \right) = w$$

Equation 12

These equations when applied with the limitation of time from $t_2 \rightarrow t_1$, we get,

$$\frac{D\rho}{Dt} = u\frac{\partial \rho}{\partial t} + v\frac{\partial \rho}{\partial t} + w\frac{\partial \rho}{\partial t} + \frac{\partial \rho}{\partial t}$$

Equation 13

This substantial derivate for coordinates in Cartesian form is as follows,

$$\frac{D}{Dt} = \frac{\partial}{\partial t} + u\frac{\partial}{\partial t} + v\frac{\partial}{\partial t} + w\frac{\partial}{\partial t}$$

Equation 14

The vector operator in Cartesian coordinates, ∇ *is* as follows,

$$\nabla = \vec{\imath}\frac{\partial}{\partial t} + \vec{\jmath}\frac{\partial}{\partial t} + \vec{k}\frac{\partial}{\partial t}$$

Equation 15

Hence, Equation 15 can be written as,

$$\frac{D}{Dt} = \frac{\partial}{\partial t} + (\vec{V}.\nabla)$$

Equation 16

With respect to the temperature T, the substantial derivative equation is notated as,

$$\frac{DT}{Dt} \equiv \frac{\partial T}{\partial t} + (\vec{V}.\nabla)$$

Equation 17

Wherein,

$$T \equiv \frac{\partial}{\partial t} + u\frac{\partial T}{\partial t} + v\frac{\partial T}{\partial t} + w\frac{\partial T}{\partial t}$$

Equation 18

www.manaraa.com

The continuity equations are derived from which Equation 19, which is split up as,

$$\underbrace{\frac{DT}{Dt}}_{Substantial\ Derivative} \equiv \underbrace{\frac{\partial T}{\partial t}}_{Local\ Derivative} + \underbrace{(\vec{V}.\nabla)}_{Convective\ Derivative}$$

Equation 19 – Substantial Derivative equation for all continuity equations

In the literature by (J.D. Anderson, 2009), a beautiful example is provided which explains the substantial derivative with the local and convective derivatives which is quoted.

"Imagine that you are hiking in the mountains, and you are about to enter a cave. The temperature inside the cave is cooler than outside. Thus, as you walk through the mouth of the cave, you feel a temperature decrease—this is analogous to the convective derivative in Equation 19. However, imagine that, at the same time, a friend throws a snowball at you such that the snowball hits you just at the same instant you pass through the mouth of the cave. You will feel an additional, but momentary, temperature drop when the snowball hits you—this is analogous to the local derivative in Equation 19. The net temperature drops you feel as you walk through the mouth of the cave is, therefore, a combination of both the act of moving into the cave, where it is cooler, and being struck by the snowball at the same instant—this net temperature drop is analogous to the substantial derivative in Equation 19."

THE CONSERVATION OF MASS

A moving infinitesimal fluid element is considered. The mass of this particle is considered to be δm and the volume is given by δV. Thus, from the equations presented by (J.D. Anderson, 2009),

$$\boldsymbol{\delta m = \rho \delta V}$$

Equation 20

As established by physics, mass is conserved and thus, the time-rate-of-change of mass of the fluid element is zero as the element moves with the flow, giving the equation,

$$\boldsymbol{\frac{D\delta m}{Dt} = 0}$$

Equation 21

Substituting $\boldsymbol{\rho \delta V}$ for $\boldsymbol{\delta m}$ in Equation 21,

$$\boldsymbol{\frac{D(\rho \delta V)}{Dt} = \delta V \frac{D\rho}{Dt} + \rho \frac{D(\delta V)}{Dt} = 0}$$

Equation 22

Or,

$$\boldsymbol{\frac{D\rho}{Dt} + \rho \left\{ \frac{1}{\delta V} \frac{D(\delta V)}{Dt} \right\} = 0}$$

Equation 23

www.manaraa.com

As discussed in the section earlier, the term in the brackets is representative of the convective derivative of the equation and thus the equation can be re-written as,

$$\boxed{\frac{D\rho}{Dt} + \rho(\vec{V}.\vec{\nabla}) = 0}$$

Equation 24 – Continuity Equation for Conservation of Mass

Equation 23 is the conservation of mass equation in non-conservation form as the fluid particles are continuously moving across the flow field.

THE CONSERVATION OF MOMENTUM

The conservation of momentum is a fundamental derived from Newton's Second Law.

$$\vec{F} = m\vec{a}$$

Equation 25

Newton's law says that the net force acting on an infinitesimal element is equal to the product of its mass times its acceleration. This can be explained by considering the following figure with a moving element. The forces related to the x – direction are shown.

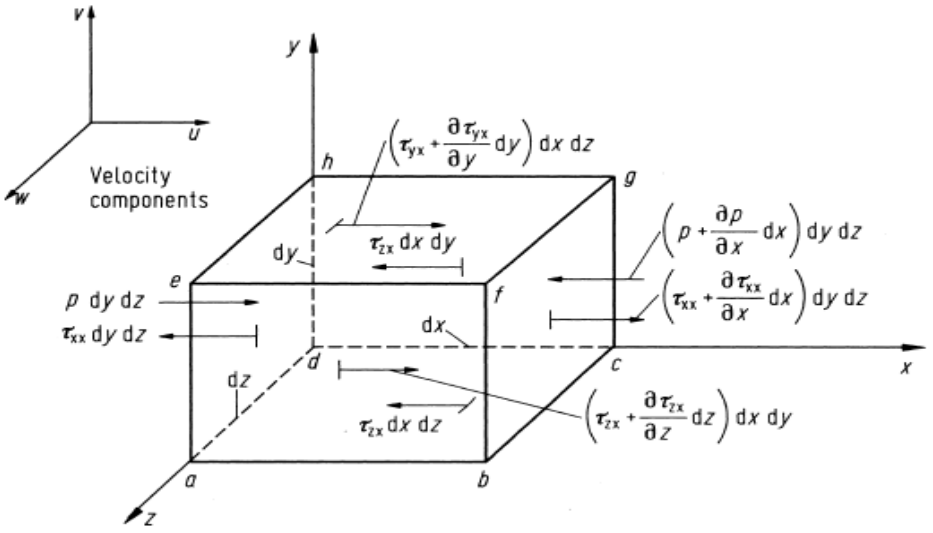

Figure 3. Infinitesimal element flowing through a 3D space (J.D. Anderson, 2009, p. 28).

Let us consider the x – component of forces,

$$F_x = ma_x$$

Equation 26

There are two types of forces acting on the body namely body forces and surface forces.

- Body forces – Gravitational, Electric and Magnetic.
- Surface forces – Pressure acting on the surface and shear & normal stresses.

www.manaraa.com

By denoting the forces acting on the body with $\vec{f}$ with f_x as its x-component and volume being $(dx\ dy\ dz)$, we get,

$$\left\{\begin{matrix}\textbf{Body force acting on}\\ \textbf{the fluid element acting}\\ \textbf{in the } x-\textbf{direction}\end{matrix}\right\} = \rho f_x (dx\ dy\ dz)$$

Equation 27

The net surface force can be written in terms of shear stress and directional components,

$$\left\{\begin{matrix}\textbf{Net surface force}\\ \textbf{in the } x-\textbf{direction}\end{matrix}\right\} =$$

$$\left[p-\left(p+\frac{\partial p}{\partial x}dx\right)\right]dy\ dz+\left[\left(\tau_{xx}+\frac{\partial \tau_{xx}}{\partial x}dx\right)-\tau_{xx}\right]dy\ dz+$$

$$\left[\left(\tau_{yx}+\frac{\partial \tau_{yx}}{\partial y}dy\right)-\tau_{yx}\right]dx\ dz+\left[\left(\tau_{zx}+\frac{\partial \tau_{zx}}{\partial z}dz\right)-\tau_{zx}\right]dx\ dy$$

Equation 28

By combining Equations 26 and 27, adding and canceling terms, we get,

$$F_x=\left(-\frac{\partial p}{\partial x}+\frac{\partial \tau_{xx}}{\partial x}+\frac{\partial \tau_{yx}}{\partial y}+\frac{\partial \tau_{zx}}{\partial z}\right)dx\ dy\ dz+\ \rho f_x(dx\ dy\ dz)$$

Equation 29

From Equation 25, we know the mass of the fluid element is fixed and is equal to,

$$m=\rho\ dx\ dy\ dz$$

Equation 30

Also, acceleration of the fluid element is the time-rate-of-change of its velocity. In the x-direction, this component is u and thus, the acceleration a is given by,

$$a_x=\frac{Du}{Dt}$$

Equation 31

Combining Equations 25, 28, 29 and 30, we get,

$$\rho\frac{Du}{Dt}=-\frac{\partial p}{\partial x}+\frac{\partial \tau_{xx}}{\partial x}+\frac{\partial \tau_{yx}}{\partial y}+\frac{\partial \tau_{zx}}{\partial z}+\ \rho f_x$$

Equation 32 Navier-Stokes Equation for momentum in X-direction

Similarly, for the y component,

$$\rho\frac{Dv}{Dt}=-\frac{\partial p}{\partial y}+\frac{\partial \tau_{xy}}{\partial x}+\frac{\partial \tau_{yy}}{\partial y}+\frac{\partial \tau_{zy}}{\partial z}+\ \rho f_y$$

Equation 33 Navier-Stokes Equation for momentum in Y-direction

www.manaraa.com

Similarly, for the z component,

$$\rho\frac{Dw}{Dt} = -\frac{\partial p}{\partial z} + \frac{\partial \tau_{xz}}{\partial x} + \frac{\partial \tau_{yz}}{\partial y} + \frac{\partial \tau_{zz}}{\partial z} + \rho f_z$$

Equation 34 Navier-Stokes Equation for momentum in Z-direction

Equations 31, 32 and 33 are the *x*, *y,* and *z* components respectively of the momentum equation in non-conservation form since the element is moving with the fluid flow.

They are scalar equations, and are called the Navier–Stokes equations in honor of two men—the Frenchman M. Navier and the Englishman G. Stokes—who independently obtained the equations in the first half of the 19th century.

K–ω MODEL

The K − ω model is gaining in popularity. The model was proposed by Wilcox (Davidson, 2016). The basic idea of the K – ω model was originated by Kolmogorov in 1942 with turbulence associated with vorticity, ω, being proportional to $\frac{K^2}{l}$ (Chung, 2002). The standard K – ω model is an empirical model based on model transport equations for the turbulence kinetic energy (k) and the specific dissipation rate (ω), which can also be thought of as the ratio of ε to k (Fluent Theory Guide, p. 4.4.1).

The turbulence kinetic energy, k, and the specific dissipation rate, ω, are obtained as,

$$\frac{\partial}{\partial t}(\rho k) + \frac{\partial}{\partial x_i}(\rho k u_i) = \frac{\partial}{\partial x_j}\left(\Gamma_k \frac{\partial k}{\partial x_j}\right) + G_k - Y_k + S_k$$

Equation 35 K- ω Turbulence Model – Transport equation for k

$$\frac{\partial}{\partial t}(\rho \omega) + \frac{\partial}{\partial x_i}(\rho \omega u_i) = \frac{\partial}{\partial x_j}\left(\Gamma_\omega \frac{\partial \omega}{\partial x_j}\right) + G_\omega - Y_\omega + S_\omega$$

Equation 36 K- ω Turbulence Model – Transport equation for ω

In these equations, G_k represents the generation of turbulence kinetic energy due to mean velocity gradients. G_ω represents the generation of ω. Γ_k and Γ_ω represent the effective diffusivity of k and ω. Y_k and Y_ω represent the dissipation of k and ω due to turbulence. S_k and S_ω are user-defined source terms.

GAMMA–RETHETA MODEL

The full transition model is based on two transport equations, one for the intermittency and one for the transition onset criteria in terms of momentum thickness Reynolds number. It is called 'Gamma Theta Model' and is the recommended transition model for general-purpose applications. It uses a new empirical correlation (Langtry and Menter) that has been developed to cover standard bypass transition as well as flows in low free-stream turbulence environments (Fluent Theory Guide, p. 2.4.1).

www.manaraa.com

The Gamma Theta Model has the following limitations:

- The Gamma Theta Model, like all other engineering transition models, is only valid for wall boundary layer flows. It cannot be applied to free shear flow transition. The model will predict free shear flows as fully turbulent.
- Due to the specific formulation of the Gamma Theta equation, only classical boundary layers with a defined freestream region can be handled. This means that the model is not applicable to situations such as a pipe or channel flow.
- The model is currently not linked to the buoyancy production terms because buoyancy driven flows are outside the calibration space of the model.
- The model is not Galilean invariant. This means it is only valid with respect to walls that are not moving relative to the coordinate system.

The transport equation for the intermittency, γ is as follows:

$$\frac{\partial(\rho\gamma)}{\partial t}+\frac{\partial(\rho U_j\gamma)}{\partial x_j}=P_{\gamma 1}-E_{\gamma 1}+P_{\gamma 2}-E_{\gamma 2}+\frac{\partial}{\partial x_j}\left[\left(\mu+\frac{\mu_t}{\sigma_\gamma}\right)\frac{\partial\gamma}{\partial x_j}\right]$$

Equation 37 Gamma Theta Turbulence Model - Transport Equation for Intermittency, γ

The transport equation for transition momentum thickness Reynolds number, $\widetilde{Re}_{\theta t}$ is,

$$\frac{\partial(\rho\widetilde{Re}_{\theta t})}{\partial t}+\frac{\partial(\rho U_j\widetilde{Re}_{\theta t})}{\partial x_j}=P_{\theta t}+\frac{\partial}{\partial x_j}\left[\sigma_{\theta t}\left((\mu+\mu_t)\frac{\partial\widetilde{Re}_{\theta t}}{\partial x_j}\right)\right]$$

Equation 38 Transport Equation for Transition Momentum Thickness Reynolds Number, $\widetilde{Re}_{\theta t}$

LANGTRY–MENTER 4–EQUATION TRANSITIONAL SST MODEL

The Transition SST model is based on the coupling of the SST K–ω transport equations with two other transport equations, one for the intermittency and one for the transition onset criteria, in terms of momentum-thickness Reynolds number (Fluent Theory Guide, p. 4.6.1).

The transition model interacts with the SST turbulence model by a small modification of the k –equation presented in Equation 35 (Menter, et al., 2006),

$$\frac{\partial}{\partial t}(\rho k)+\frac{\partial}{\partial x_i}(\rho k u_i)=\frac{\partial}{\partial x_j}\left(\Gamma_k\frac{\partial k}{\partial x_j}\right)+G_k^*-Y_k^*+S_k$$

Equation 39

$$G_k^*=\gamma_{eff}\widetilde{G}_k$$

Equation 40

$$Y_k^*=min\left(max\left(\gamma_{eff},0.1\right),1.0\right)Y_k$$

Equation 41

www.manaraa.com

Where $\widetilde{G}_k$ and Y_k are the production and destruction terms from the turbulent kinetic energy equation in the original SST turbulence model and γ_{eff} is the effective intermittency. The production term in the ω - equation is not modified.

COMPUTATIONAL FLUID DYNAMICS – MODELING

According to the National Training and Simulations Association, "Modeling is the representation of an object or phenomena, which is used by simulations" (National Training and Simulation Association , 2011, p. 3). "In fact, models may be mathematical, physical or logical representations of a system, entity, phenomenon or process, or a combination of two or more of these. Moreover, a model can also be a system with integrated functions constructed in completely an artificial environment. Hence, the only thing that distinguishes a model from reality is that it should be comparable but simpler than a real system" (Kankanamge, 2015, p. 6).

Creating a model with an approximation of the system is the first step of an M&S system. Then, the model can be modified according to the experimental procedure desired (Sokolowski & Banks, 2010, p. 1). In other words, the main object of a model is to forecast or predict the outcome of an alteration of the system (Maria, 1997, p. 7).

Modeling is performed in two variants namely physical modeling and mathematical modeling. This thesis utilizes both these systems. Primarily, mathematical models are utilized to predict the functionality of the real world application in a computational environment. Physical models are used to validate the results of the computational study.

Figure 4. Comparison between a Mathematical (CAD) Model and a Physical Model.

www.manaraa.com

COMPUTATIONAL FLUID DYNAMICS – MESHING

The first step in the Finite Volume Method is to divide the domain into discrete control volumes (Versteeg & Malalasekara, 1995, p. 86). The basic idea is to make calculations at only limited (Finite) number of points and then interpolate the results for the entire domain (surface or volume) (Nitin & Lee, 2008, p. 1). The mesh generation is the process of breaking down the fluid domain into a number of smaller, non-overlapping subdomains (Tu & Guan Heng, 2007, p. 35). Generally, mesh generation starts at the edges, and then moves to the faces, and finally to the volume of the domain (Wendt, Anderson, & Von Karman Institute, 2008, p. 310).

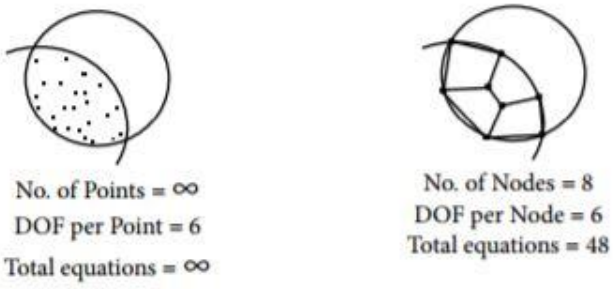

Figure 5. Importance of Meshing (Nitin & Lee, 2008).

There are three types of grids commonly used in analytical applications. They are namely unstructured mesh, structured mesh, and hybrid mesh. When large blocks of a fluid domain are broken down to into discrete cells, it is called structured mesh generation. In the same manner, when variable cells are directly surrounded by complex geometric domains, it is called unstructured mesh generation (Kleinstreuer, 2010, p. 527).

The mesh for any domain must be a function of the user's requirements and computational resource power availability. The solution of a computational problem is only as good as its grid generation process is. Typically, researchers spend about 25-50% of their time on creating the right mesh to fulfill their needs for obtaining exact solutions. Thus, to have accurate results, one must model the computational fluid domain with a greater number of elements at the "region of interest" and check the mesh quality which can be measured by methods such as Skewness, Aspect ratio and Jacobian Warping factor.

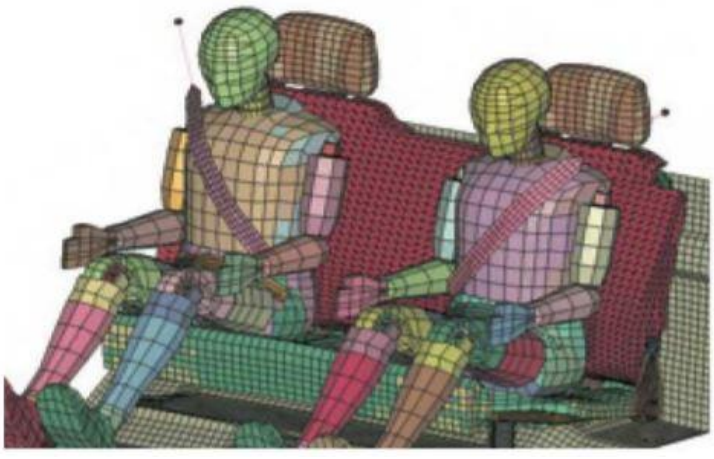

Figure 6. Demonstration of a 3D Mesh. Courtesy: Tata Johnson Controls Automotive Limited, India.

www.manaraa.com

COMPUTATIONAL FLUID DYNAMICS – SIMULATION SETUP

Simulation Setup is the process of setting up the physics of the problem, the fluid characteristics, boundary conditions and the solver criteria. The method includes the tasks of providing a set of algebraic equations for the unknowns and prescribing an algorithm for solving these equations (Suhas, 1980, p. 26). It is a very crucial step which directly impacts the results of the computational simulation. Thus, the user needs to have significant knowledge of the extent of the problem's scope and the expected results.

Boundary conditions are defined on each face of a three-dimensional model and each edge of a two-dimensional model (Kleinstreuer, 2010, p. 527). The purpose of the boundary conditions is to define the flow field within the boundaries of the flow region and to mimic the actual physical representation of the application (Wendt, Anderson, & Von Karman Institute, 2008, p. 306).

The solver criterion includes initializing the solution and monitoring the convergence of the problem. Computational fluid dynamics utilize a set of partial difference equation to solve the flow field properties such as velocity and pressure iteratively. The initialization provides an initial estimate of the final solution to the solver. If improper initial conditions are used, the convergence process can be disorganized; resulting in higher computational times or incorrect results (Tu & Guan Heng, 2007, p. 47).

"Convergence is the process used to determine the point at which the solution to the algebraic equations is close to that of the partial differential equations. Convergence is achieved by monitoring the imbalance or residuals brought forward by the numerical calculations of each iteration step. These imbalances reflect and report the global flow property conservation to the CFD tool" (Kankanamge, 2015, p. 62). A final result is obtained once the residuals fall below the convergence criteria provided by the user.

COMPUTATIONAL FLUID DYNAMICS – POST PROCESSING

The final step in a CFD simulation process is to visualize and analyze the results produced by the computational analysis solution. Many colorful and informative animations and pictures can be generated to visualize flows, streamlines, and areas of significance. The various plots that can be used are contour plots, vector plots, XY scatters and streamlines plots. Flow animations can also be produced to view particle motion as a function of time.

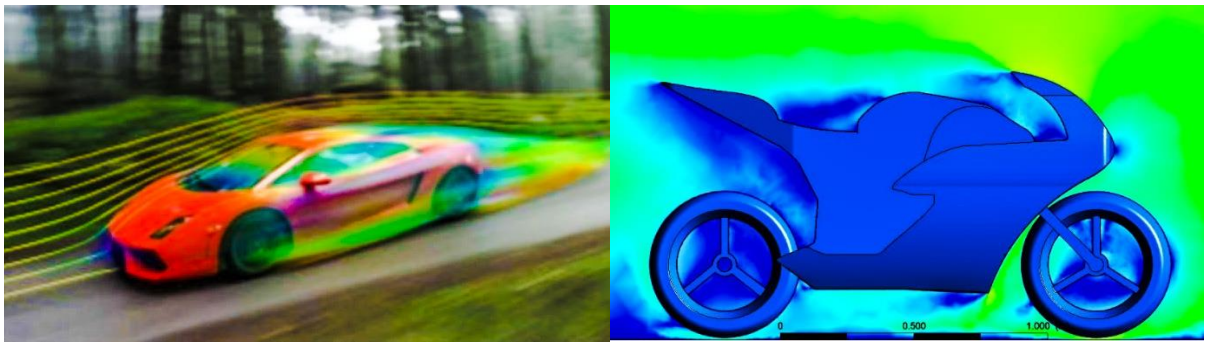

Figure 7. Snapshots of Post Processing Results Using Streamline and Contour Plots (T.M.V Engineering Blog, n.d.).

www.manaraa.com

CHAPTER 3 – DESIGN AND MODELING

THE DESIGN PROCESS

The first step in a computational study is to assess the design of the various concepts involved. Designing involves analyzing the body of interest, the impact areas associated with research, the simplicity of design and the relevance of the design to the real world.

In the case of the thesis, the body of interest is the motorcycle model, the airfoils for the modification concept of active aerodynamics being tested and the wind tunnel used for testing. Thus, the design process includes the sub-sections describing the generation of a mathematical model for the motorcycle, the airfoils, the assembly of these two design components to replicate the various phases of active aerodynamics on the motorcycle and the modeling of the wind tunnel to replicate the actual wind tunnel.

THE MOTORCYCLE

The motorcycle's design was split up into multiple phases. Primarily, a background picture was chosen to sketch up the model. This was followed by extracting individual components of the motorcycle body through design functions. Finally, the last step included refining the model to promote better aerodynamics and overall aesthetics. The original model was scaled down to a 1:10 scale to perform experimentation.

BACKGROUND PICTURES AND SKETCH UP

The motorcycle sample model chosen to sketch up the initial outline of the CAD model was a 2005 Honda CBR 1000RR Fireblade. This is the most appealing motorcycle to the author of this thesis. Two pictures, one for the side view and one for the front view were used to sketch up the 3D CAD model. The pictures utilized are as follows.

Figure 8. Pictures of the Side and the Front View of a 2005 Honda CBR1000RR Fireblade (MCN Bikes For Sale, n.d.).

www.manaraa.com

These pictures were imported into the software PTC Creo V3.0. The following steps were used to insert the pictures into the 3D space.

PTC Creo V3.0 ➔ View Tab ➔ Model Display ➔ Images ➔ Select Plane ➔ Import

The picture of the side view of the motorcycle was placed on the left plane of the 3D space. The front view was placed in the front plane of the 3D space. The 3D space with the pictures inserted into the respective planes appeared as follows.

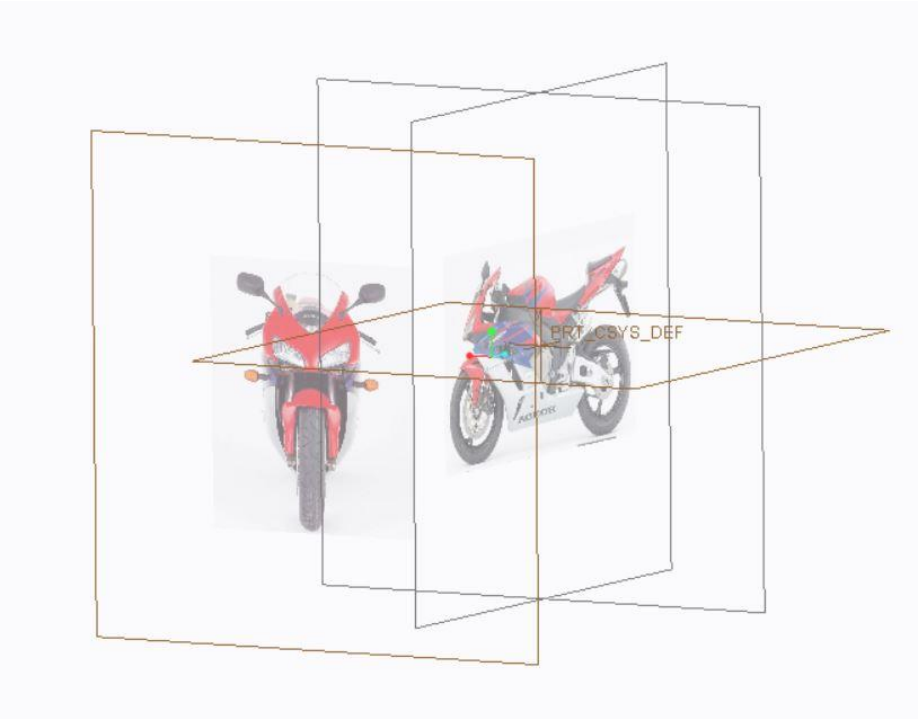

Figure 9. Snapshot of the PTC Creo V 3.0 User 3D Space with Reference Images in Planes.

Once the pictures were inserted, the outlines for the various components such as the fairing, the tank, the tail and the wheels were sketched separately with reference surfaces of extruded components being used to sketch the subsequent components. A few snapshots of the sketching process using the reference pictures are shown as follows.

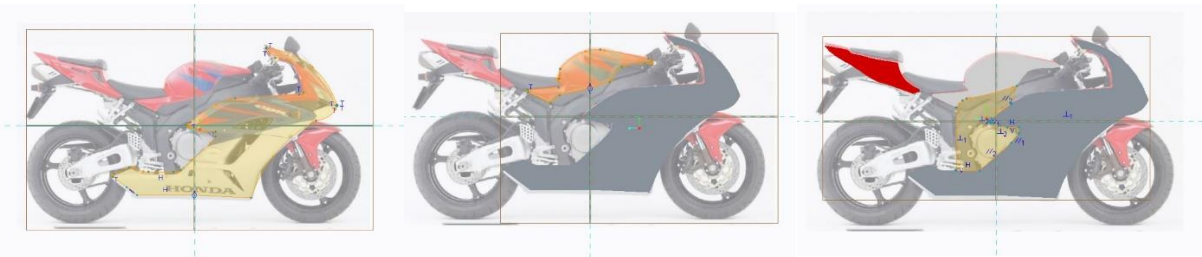

Figure 10. LEFT – Fairing Sketch-Up. RIGHT - Engine Area Sketch-Up using the Extruded Fairing as Reference.

www.manaraa.com

Each sketch was extruded in the side view. The front view was used to carve the detailing for the 3-Dimensional view of the motorcycle. This process was continued until the entire CAD model was designed to an acceptable level of mechanical detailing.

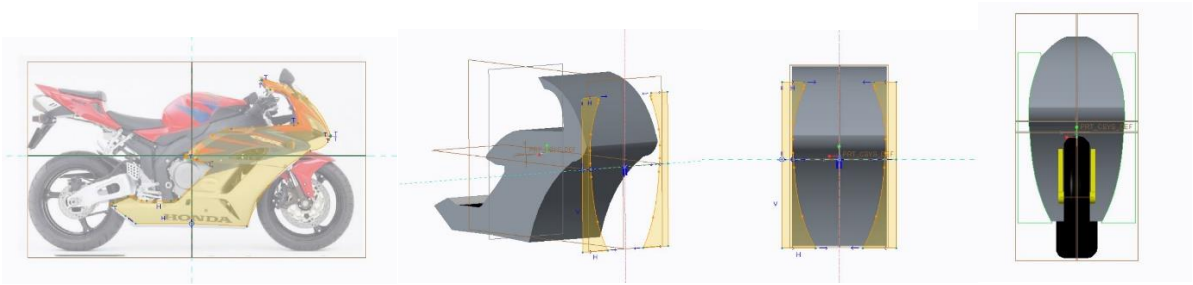

Figure 11. Sketch-Up (Using Side View) ➔ Extrude ➔ Carve (Using Front View) Design Process in Pictures.

REFINING THE MOTORCYCLE MODEL

The completed CAD model was subject to refinement to improve the aerodynamic characteristics and to promote better aesthetics. Few key functions performed as a part of the refinement process were as follows:

- Rounding and Smoothing: Rough edges hinder good airflow. Rounding and smoothing these edges presents a smoother surface for the airflow, thereby reducing aerodynamic drag. (Function used in CREO: Round and Auto-Round).
- Closure of Gaps and Voids: Gaps and voids in a CAD model will present a wide array of issues to a computational study of external flow aerodynamic analysis. The software analyses these gaps and voids as entities within the flow field and will flow the air through these empty spaces. This will increase the turbulence which is unexpected by the user and increases the Drag Coefficient of the model.
- Producing Key Aerodynamic Features: Key features such as headlamps and frontal fairing area were modified. The front of the motorcycle was focused on as this is the area that the airflow causes a primary major impact. Thus, a successful attempt was made to design the fairing as a surface that promoted smooth airflow with a smooth curvature. The headlamps were integrated into the surface as well.

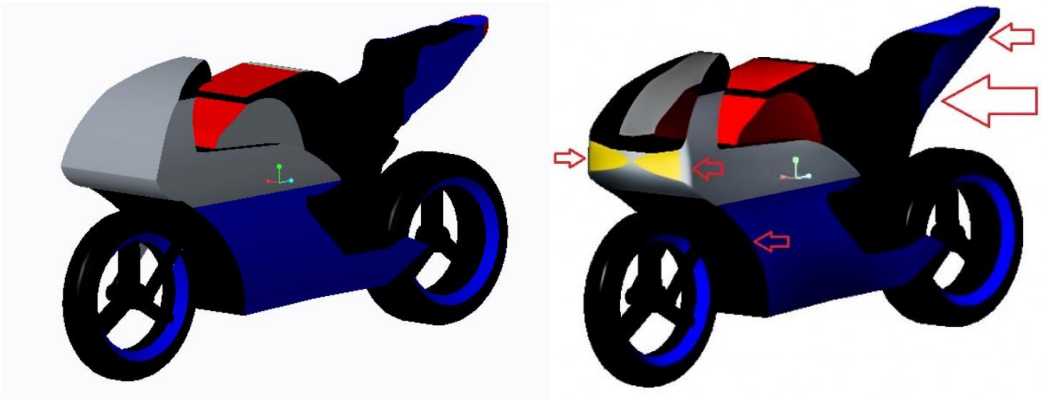

Figure 12. Refinements - Headlamps, Rounded Fairing Edges, Front-End Modified, and Tail-End Straightened.

www.manaraa.com

THE AIRFOILS

The airfoil used for the project was a NACA 6412 IL airfoil. The airfoil was chosen for the project as it had high camber on both the top and the bottom surfaces. Restrictions on wing size to be used was a key factor in deciding the choice of the airfoil. Thus, an airfoil that could produce great downforce even at small airfoil area due to the camber was chosen appropriately for the project. The NACA 6412 IL airfoil profile is as follows:

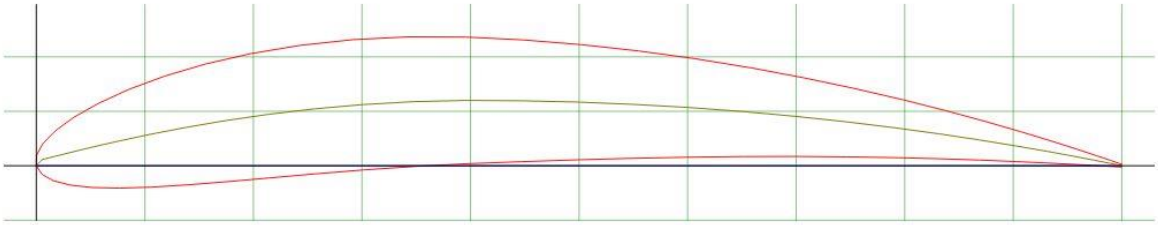

Figure 13. NACA 6412 IL Airfoil Profile (UIUC Airfoil Coordinates Database, n.d.).

The airfoils are primarily used in aerospace applications, thus they bear a resemblance in profile as shown above. They are primarily used to generate lift. Lift is a mechanical force that is generated by a solid object moving through a fluid (Hall, 2015). Lift occurs when a moving flow of gas is turned by a solid object. The flow is turned in one direction, and the lift is generated in the opposite direction, according to Newton's Third Law of action and reaction (Hall, 2015). In the case of automotive applications, the downforce is a significant factor. This is produced when the airfoil is turned upside down. An illustration is made to show the difference between lift and downforce.

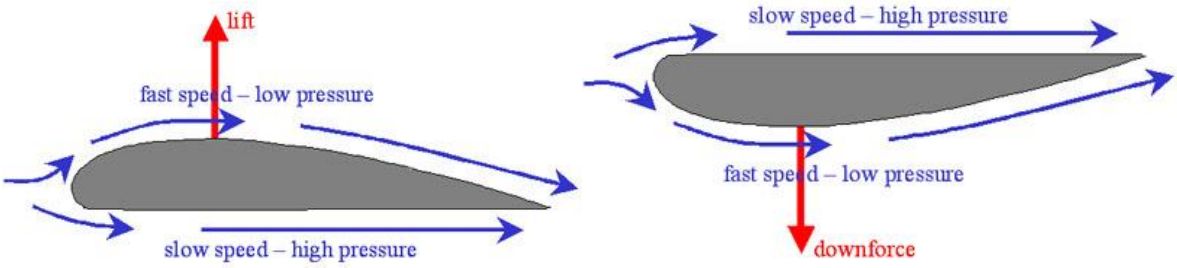

Figure 14. The difference between Lift and Downforce produced by an Airfoil.

Thus, to design the airfoil, the coordinates were imported from the website and pasted into the form of an Excel sheet. In CREO, two splines were drawn and edited by importing the coordinates of the top and bottom curves of the airfoil. The chord length i.e., the distance between the leading and trailing edge of the airfoil was chosen as 10cms. Once the sketch was drawn, the airfoil was extruded for a span length of 15cms. The effective area of the airfoil was 150cm^2 originally. For final computational research and experimentation, a scaled-down version of the original model by a 1:10 Scale were used.

www.manaraa.com

THE MOTORCYCLE-AIRFOIL ASSEMBLIES

To design the concept of active aerodynamics, the airfoils needed to be actuated at various angles. A point of assembly was chosen based on simulations conducted to assess the point of optimal airflow velocity. Since the key here was to simulate downforce production during acceleration and drag force production under braking, four different models were chosen. The attack angles chosen for downforce production were 0° and 10°. The attack angle chosen for drag force production was 90°. The four models were:

- Non-Wing Motorcycle Model: The Motorcycle was used without any wings.
- 0° Wing Motorcycle Model: The airfoil was mounted at a 0° attack angle.
- 10° Wing Motorcycle Model: The airfoil was mounted at a 10° attack angle.
- 90° Wing Motorcycle Model: The airfoil was mounted at a 90° attack angle.

The final CAD models are as shown in the pictures below.

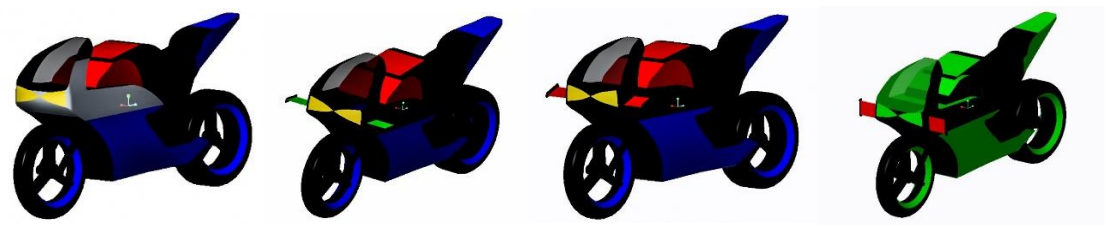

Figure 15. LEFT TO RIGHT - Non-Wing, 0 Degrees, 10 Degrees and 90 Degrees CAD models.

THE WIND TUNNEL

The Wind Tunnel was mathematically modeled utilizing the dimensions from the actual Wind Tunnel located in the Wind Tunnel Laboratory at Minnesota State University, Mankato. The dimensions were 90cms*30cms*30cms. The mathematical model also accounted for the flow properties of the wind tunnel. The inlet was termed as a Velocity Inlet, the outlet was a Pressure Outlet and the walls of the wind tunnel were termed as Wall Symmetries. The motorcycle was termed as the Motorcycle Wall Boundary.

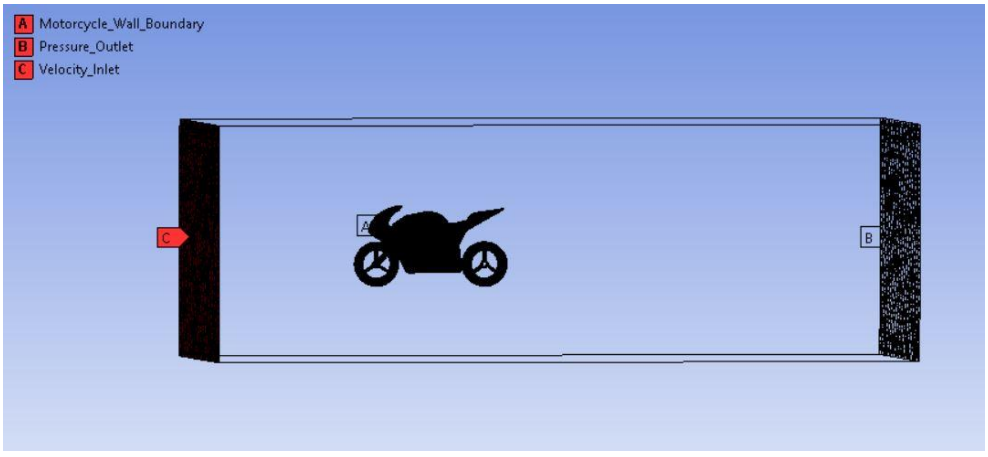

Figure 16. Virtual Wind Tunnel CAD Model with Motorcycle CAD Model.

www.manaraa.com

CHAPTER 4 – COMPUTATIONAL RESEARCH

The computational research process involved working with computer tools to produce a simulated result for the thesis' concept. The primary tool used during the computational research phase was ANSYS Workbench V17.2 Academic. The various modules used during the computational phase in ANSYS Workbench were ANSYS Design Modeller, ANSYS Mesh, ICEM CFD, ANSYS Fluent and ANSYS Post Processing. All work was performed on a 1:10 Scale model designed using computer tools as mentioned in the previous chapter. The sub-chapters of the computational research section are also divided based on the four main elements of a CFD Simulation i.e. Pre-processor or grid setup, Simulation Setup i.e. Transport Equation and sub model parameter setup, Solver setting to solve transport equations i.e. Analyze results and Post Processing (Chakrabarty, Mannan, & Cagin, 2015, p. 211).

PRE-PROCESSING

As discussed in the introductory chapter, pre-processing or mesh generation is the process of breaking down the fluid domain into a number of smaller, non-overlapping subdomains (Tu & Guan Heng, 2007, p. 35). The pre-processing is performed after the design process is completed. There are three types of popular meshing methods that are utilized. In the case of the thesis, as the geometry was a complex CAD model of a motorcycle, the unstructured mesh was used to carefully mesh the domain. The benefit of using an unstructured mesh, in this case, is reducing the time spent on meshing and providing flexibility to the user. The specific tool used in this case in the ANSYS Mesh tool. Snapshots of the pre-processing are illustrated below to provide a general understanding.

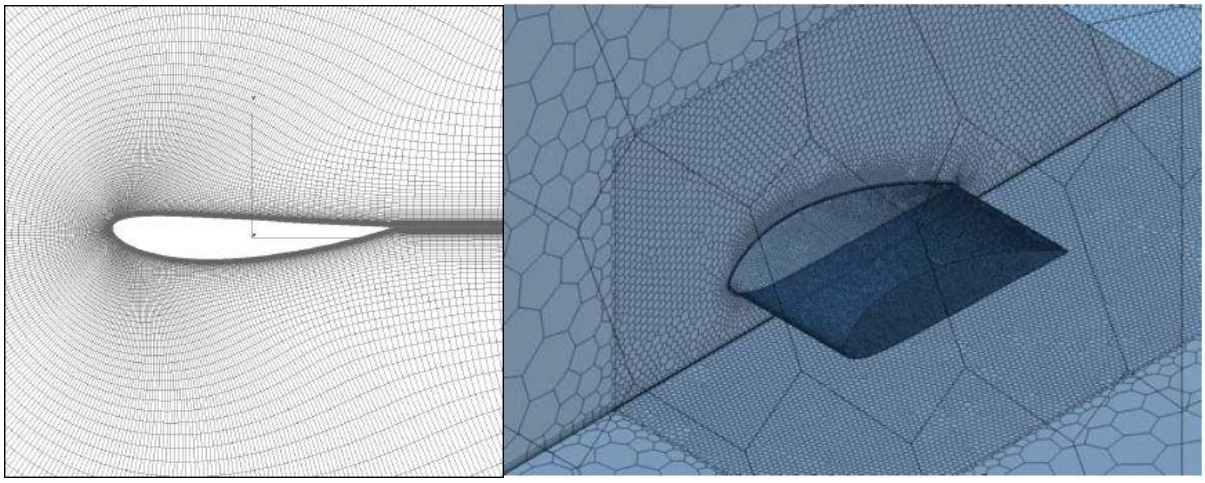

Figure 17. LEFT: C Type Hyperbolic Grid Mesh (Thisse, 2004). RIGHT: Polyhedral Mesh (Park, Hong, Kim, & Lee, 2008).

For the thesis, the mesh consisted of unstructured elements. The mathematical model consisted of a motorcycle (with airfoils) inside of a wind tunnel CAD model. The wind tunnel fluid domain was modeled with elements of a greater size. The motorcycle body was assigned a local sizing of 5mm to generate detailed results at the body of interest. In doing so, the processor effort reduces and only the areas of interest are computed with greater detail to provide accurate results.

www.manaraa.com

The metric for evaluating the mesh quality was chosen as the element skewness. Equiangular Skew is the measure of an element's skewness corresponding to an equilateral triangle of similar form (Sun, 2007). It is a value ranging from 0 to 1, the smaller the better, and, as a guideline, elements of skewness of more than 0.95 are considered unacceptable (Lee, 2014, p. 327).

The final mesh consisted of 4 Million elements with a maximum skewness of 0.84. Fluent accepts maximum element skewness of up to 0.90 for result computation although having a lower skewness value is a key indicator of a good mesh. The result is as follows.

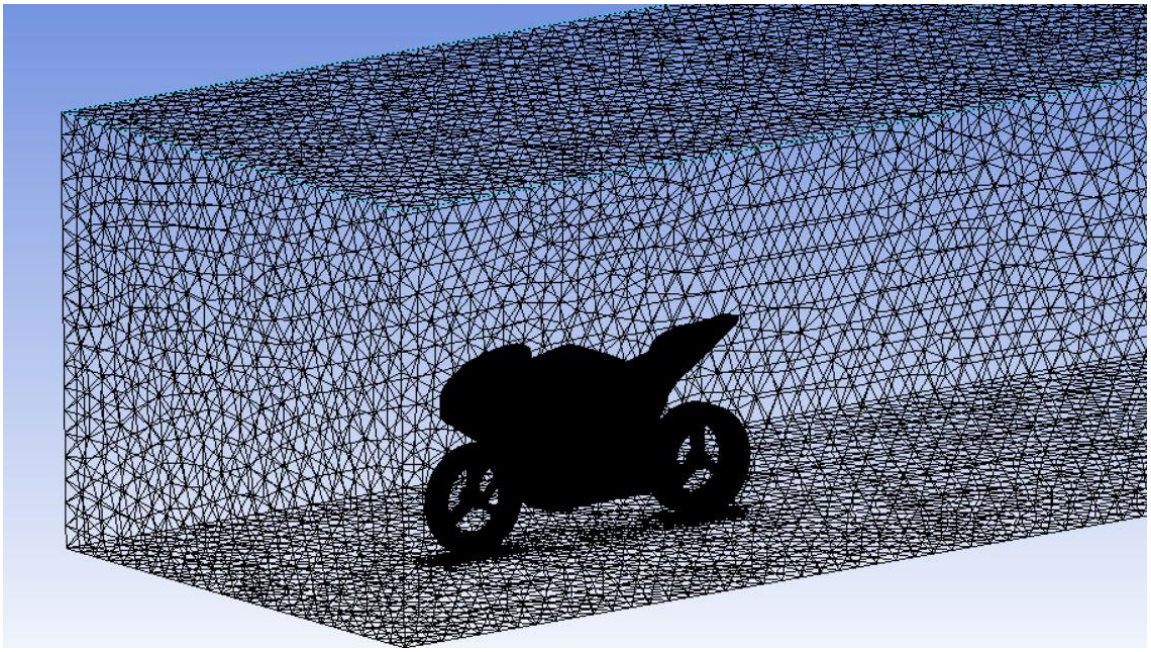

Figure 18. 3D Unstructured Grid Mesh with Sizing of 5mm at the Motorcycle Body (Region of Interest).

SIMULATION SETUP

The simulation setup is the step where the actual parameters of the simulation are to be set up for the solver. The specific tool used for this section is ANSYS Fluent. The key aspects of the simulation setup process include:

- Assigning model properties such as Air flow nature, heat transfer, energy etc.
- Materials to different areas of the domain as required.
- Boundary conditions such as inlets, outlets, and walls.
- Reference Values for the areas of interest being inspected.
- Solution Methods for improving the discretization process.
- Assigning monitors for monitoring the $\boldsymbol{C_L}$ and $\boldsymbol{C_D}$.
- Initialization to provide an initial estimate of the final solution to the solver.
- Setting up the calculation's run time or number of iterations.

www.manaraa.com

In the case of the thesis, the input details of the above-mentioned steps are as follows:

Parameter	Input Sections	User Input
Model Properties	Viscous	Transition SST 4 Equation
Materials	Fluid	Air
	Solid	Aluminium
Boundary Conditions	Velocity Inlet	Magnitude = 44.704 m/s.
		Turbulent Intensity = 5% at a Length Scale of 0.3m.
Reference Values	Area	Lifting Area for Lift. Frontal Area for Drag
	Density	1.225 kg/m^3
	Length	0.3m
	Temperature	288.16K
	Velocity	44.704m/s
Monitors	Residuals, Statistic and Forces	C_L and C_D monitors
Solution Initialization	Check boxes	Hybrid Initialization
Calculations Activities	Check case; Iteration count.	Checked; 500 iterations.

Table 1. Simulation Setup Parameters in ANSYS Fluent for the Thesis.

ANALYSIS OF COMPUTATIONAL RESULTS

The output from ANSYS Fluent is provided mainly in terms of two variables. These are the Coefficient of Lift (C_L) and Coefficient of Drag (C_D). These two values are used to calculate the basic forces of Lift and Drag over the motorcycle. The simulations were conducted on the four concept models i.e. Non-Wing model, 0 Degree Wing mode, 10 Degree Wing model and 90 Degree Wing model. All models were simulated at the 1:10 scale size as mentioned previously. The values obtained were as follows.

Model Name	C_L	C_D
Non-Wing	0.0562908	0.548149
0 Degree Wing	0.0553119	0.515643
10 Degree Wing	-0.0140432	0.532837
90 Degree Wing	N/A	0.612721

Table 2. Table of Coefficients of Lift and Drag obtained from ANSYS Fluent.

www.manaraa.com

Forces were calculated using the formulae for Lift and Drag. The parameters used to calculate lift were the velocity, lifting area, density and coefficient of lift. The parameters used to calculate drag were the velocity, frontal area, density and coefficient of drag. The forces were obtained in Newton and were converted into KgF. The forces obtained for all models are as shown in the table below.

Model Name	Density (ρ) (Kg/m^3)	Area (A_L & A_D) (m^2)	Velocity (V) (In m/s)	Lift Force (F_L) (In KgF)	Drag Force (F_D) (In KgF)
Non-Wing	1.225	A_L = 0.00675 A_D = 0.00379	44.704	0.04682	0.25626
0 Degree Wing	1.225	A_L = 0.00683 A_D = 0.00380	44.704	0.04659	0.24133
10 Degree Wing	1.225	A_L = 0.00681 A_D = 0.00404	44.704	-0.01178	0.26513
90 Degree Wing	1.225	A_L = N/A A_D = 0.00390	44.704	N/A	0.29496

Table 3. Lift and Drag Forces on all models obtained through CFD Testing.

POST PROCESSING AND VISUALIZATIONS

Various methods were used to visualize the results of the CFD simulations. Streamline flows, Contour plots for pressure & velocity and Vector flows were used. The various plots are presented in a sequence below for clearer visualization. All these plots show the various areas of aerodynamic significance on the motorcycle.

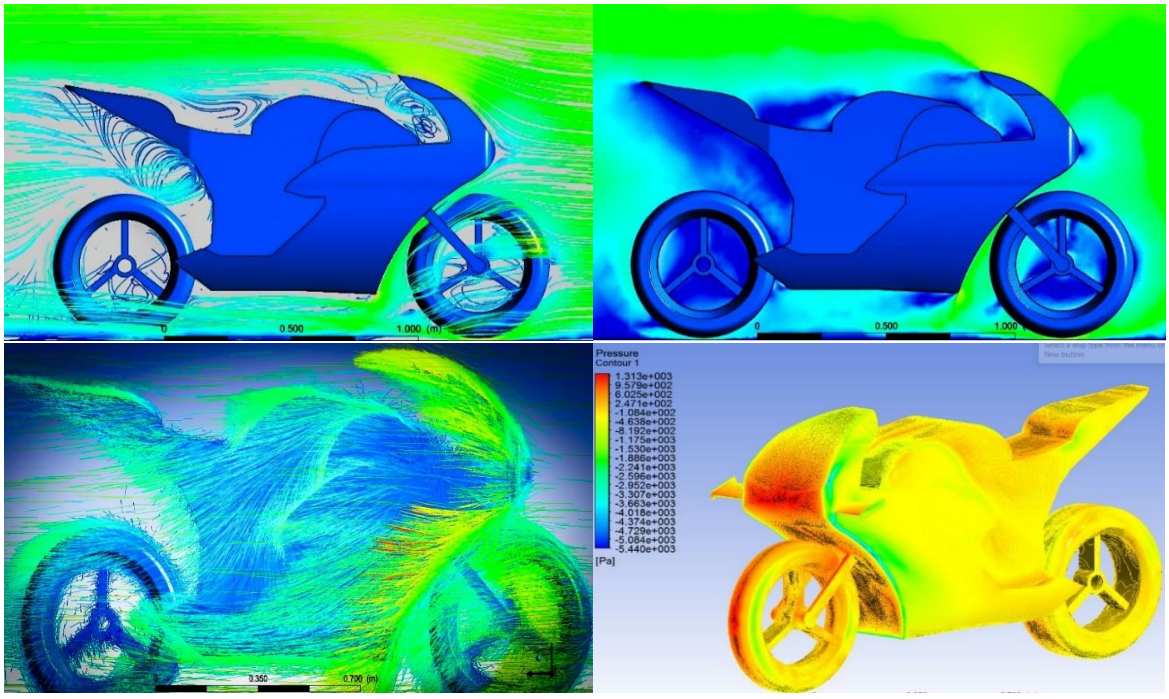

Figure 19. FROM TOP LEFT CLOCKWISE: Streamline Plot, Velocity Contour, Pressure Contour and Vector Plot.

www.manaraa.com

CHAPTER 5 – PRODUCTION PROCESS

To verify the data from the computational study, a real-world test or a validation test is required. Thus, a wind tunnel study of the proof of concept was planned. The idea was to test all the design models in the wind tunnel. Hence to achieve this, the requirement of manufacturing prototypes arose. Due to its robust nature, no need for costly tools, molds, or punches, no scrap, milling, or sanding requirements, automated manufacturing and speed and ease of designing and modifying products (Berman, 2011), 3D printing was identified as the desired process for producing the prototypes.

The 3D printer utilized was a Stratasys U-Print. It was coupled with their software named CatalystEX. The process of importing the CAD model was done through PTC Creo. 3D models designed in PTC Creo were saved in the format of a STEP (STandard for the Exchange of Product model data) file, a new International Standard (ISO 10303) for representing and exchanging product model information (CAE Users). These STEP files were then scaled down to the 1:10 size and saved as an STL (Stereolithographic) file.

Once imported, the general check-up would be performed on the model and support material for building the structure. The model would be oriented in the required direction and saved as a CMB file and would be added to the pack. The print command on the software and the Stratasys U-Print 3D printer would be activated to begin the printing process. Once the 3D printing process finished, the models would be put in an acetone bath to remove the support material. All four models namely the non-wing, 0-degree wing, 10-degree wing and 90-degree wing were manufactured separately to aid in faster transitioning between tests in the wind tunnel. The final 3D printed models were polished and spray painted in black color for flow visualization in the wind tunnel.

Figure 20. Finalized 3D Printed Models. FROM LEFT: Non-Wing, 0 Degrees, 10 Degrees and 90 Degrees Models.

www.manaraa.com

CHAPTER 6 – WIND TUNNEL TESTING

The completion of the computational testing phase yielded results that were both quantitative and qualitative. The quantitative data produced included lift and drag force figures representative of the physical forces acting on the body. The qualitative data was of the various flow visualizations that were performed in the CFD post-processor. All the data put together gave us an initial picture of the working proof of the concept.

With the 3D printed models ready for wind tunnel testing, the ELD wind tunnel in Trafton East TE 104 laboratory at Minnesota State University, Mankato was setup. The ELD (Engineering Laboratory Design, Inc.) Wind Tunnel Instrumentation System is a complete basic instrument package that has been designed for use with subsonic wind tunnels in undergraduate student laboratories. The functions of the system include the measurements of lift and drag forces, static and dynamic pressures, and the reporting of the streamwise and vertical position (X and Y coordinates) of a traversing probe (Engineering Laboratory Design, 2007, p. 1).

The wind tunnel measured 30cm wide and 30cm tall with a length of 90cm. Peak velocity of airflow in the wind tunnel was 150fps or 45.7m/s. Forces generated by the model under test are conveyed to the dynamometer via a stiff strut and result in the deflection of the beam assemblies. These deflections are proportional (within range) to the magnitude of the applied forces. The detection of each beam assembly is sensed by a Linear Voltage Displacement Transducer (LVDT) (Engineering Laboratory Design, 2007). The prototypes were mounted on top of the strut through the use of a mounting fixture.

Two key functions needed validation in the wind tunnel. Primarily, the quantitative CFD data needed verification. To verify this, the electronic data display system was utilized which displayed the forces acting on the body in the wind tunnel.

In addition to this, the qualitative data also could be verified providing further evidence to satisfy the claims of a successful concept. To aid in this process, a SAI Bubble Generator Setup was utilized. The SAI Model 5 Bubble Generator provides a compact and unique tool for visualizing complex airflow patterns. Helium-filled, neutrally-buoyant bubbles of uniform size, adjustable from 1/32" to 3/16" in diameter, can be generated simultaneously from one or two "Heads". These bubbles are capable of tracing intricate air motions without bursting or impacting on objects within the airflow (Sage Action, 2002, p. 1). This system was used to visualizing the various flows over the prototypes.

QUANTITATIVE TESTING

The quantitative testing was performed to evaluate the actual forces acting on the prototypes. The forces were classified as lift force and drag force. Measurements were put out at a velocity of 44.7m/s in correlation to the CFD study. The forces (in KgF) acting on the motorcycle models were as follows.

www.manaraa.com

Model Name	Lift Force	Drag Force
Non-Wing	0.046	0.274
0 Degree Wing	0.046	0.265
10 Degree Wing	-0.011	0.288
90 Degree Wing	N/A	0.329

Table 4. Lift and Drag Forces on all models obtained through Wind Tunnel Testing.

QUALITATIVE TESTING

The qualitative testing provided some exclusive details into the accuracy of the CFD results. Two primary aerodynamic characteristics were visualized; streamline flows and the vortex core region. The streamline flow was visualized at four different points on the prototype; near the headlamp area, at the void behind the windblast, under the tail section and over the wing sections along the wingtips. The following images illustrate the phenomenon neatly in sequence from the headlamp to the tail section.

Figure 21. Visualization Testing using the Wind Tunnel. LEFT: Headlamp area showing the flow separation, the stagnation point and vortices behind the windblast area. RIGHT: Tail end vortices a.k.a. Wake of the Motorcycle.

Thus, this completed the final step of the experimentation of the thesis. The next chapter deals with the analyses of the various outcomes of both the CFD study and the Wind Tunnel testing. Key comparisons, contrasting information, and validity of the study are discussed as results and are followed by the recommendations for future studies.

www.manaraa.com

CHAPTER 7 – ANALYSES AND RESULTS

This chapter of this thesis report deals with the analyses of the collected data. In a similar fashion, this chapter is also divided into two main sections namely Quantitative Data and Qualitative Data. The comparisons between the CFD study and the Wind Tunnel Validation are performed to provide final results for the study.

QUANTITATIVE STUDY

The quantitative study provides us with two sets of data, one from the CFD and the other from the Wind Tunnel. Comparing these data sets in a single table enables a clearer interpretation of the validity of the results. The cumulative data table is as follows.

Model Name	Lift (CFD)	Lift (Wind Tunnel)	Drag (CFD)	Drag (Wind Tunnel)
Non-Wing	0.04682	0.046	0.25626	0.274
0 Degree Wing	0.04659	0.046	0.24133	0.265
10 Degree Wing	-0.01178	-0.011	0.26513	0.288
90 Degree Wing	N/A	N/A	0.29496	0.329

Table 5. Comparison of Results between CFD and Wind Tunnel Forces Data.

As one can observe, the correlation between the lift forces obtained with the CFD and the Wind Tunnel holds good up to the third decimal with the correlation study performed in Microsoft Excel producing a correlation value of 0.999995 showing that indeed the data is fully correlative with regards to the lift estimation in CFD vs. Wind Tunnel Testing.

In the case of the drag, the predicted drag (CFD) vs. the observed drag (Wind Tunnel) has a slight deviation across all the models. The correlation study performed in Microsoft Excel produced a correlation value of 0.981791 meaning there was an error of approximately 2% indicating that the experiments are in strong correlation. As much as 20–30% of this difference is attributable to viscous forces included in predictions but absent from test data (Romander, Norman, & Chang, 2011).

In general, the drag coefficient tends to be over-predicted when the air velocity increases, which means that the faster the stream is flown, the larger the relative error gets between the wind tunnel experiments (Varela-Boydo & Castro-Gómez, 2015, p. 305). In this case, there is an under prediction or in other words an over observed drag. The data, however, shows that the CFD formed here is very approximate to the real world observations.

www.manaraa.com

QUALITATIVE STUDY

The qualitative study produced visual results that were used as a second mode of validation of the CFD results. ANSYS Post-processing software is capable of producing very highly detailed streamline, contour, and vector plots. The wind tunnel streamlines testing produced streamlines and vortex core regions for visualizations.

The CFD results were compared with the Wind Tunnel testing in two aspects; streamline plots and vortex core region formation. The various comparisons and their accuracy are depicted in pictures as follows.

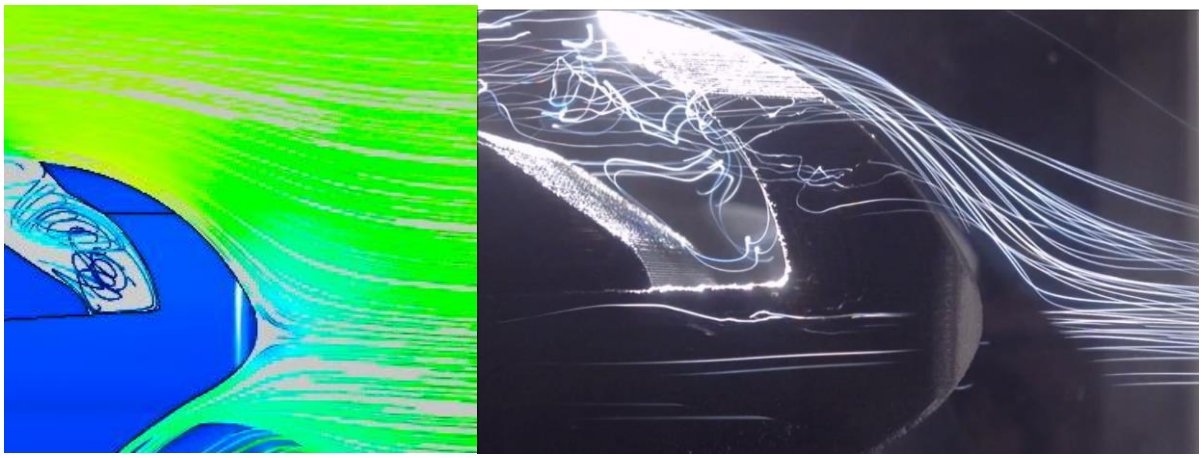

Figure 22. Validation of CFD Results: Stagnation Point at the Front, Vortices behind Windshield.

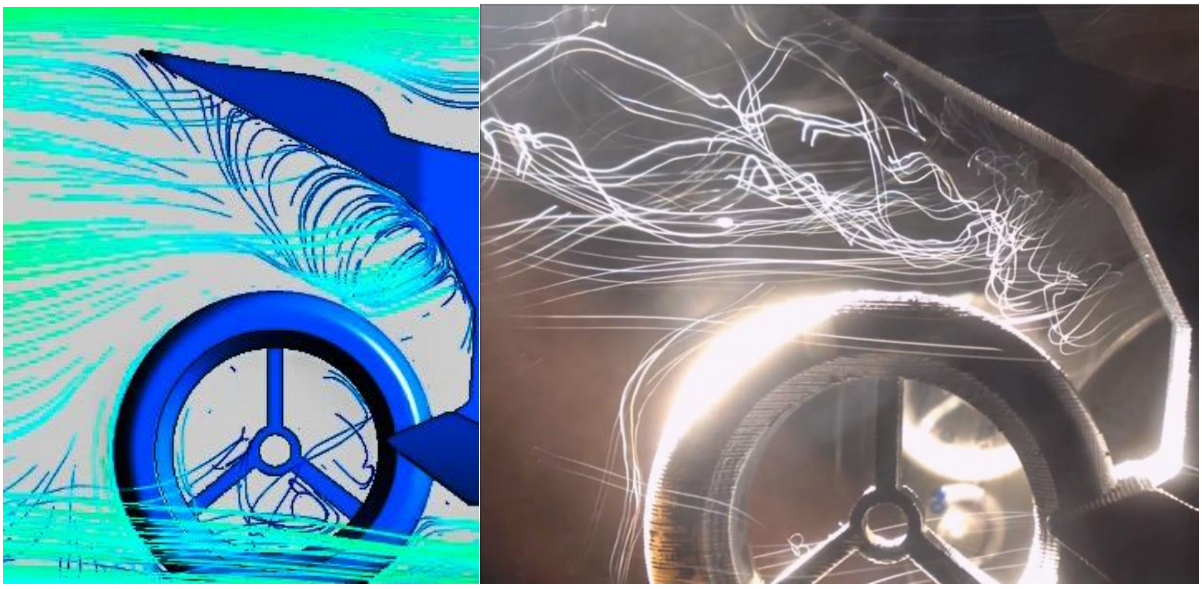

Figure 23. Validation of CFD Results: Vortices Formation under Tail Section and Streamlines behind the Wheel.

www.manaraa.com

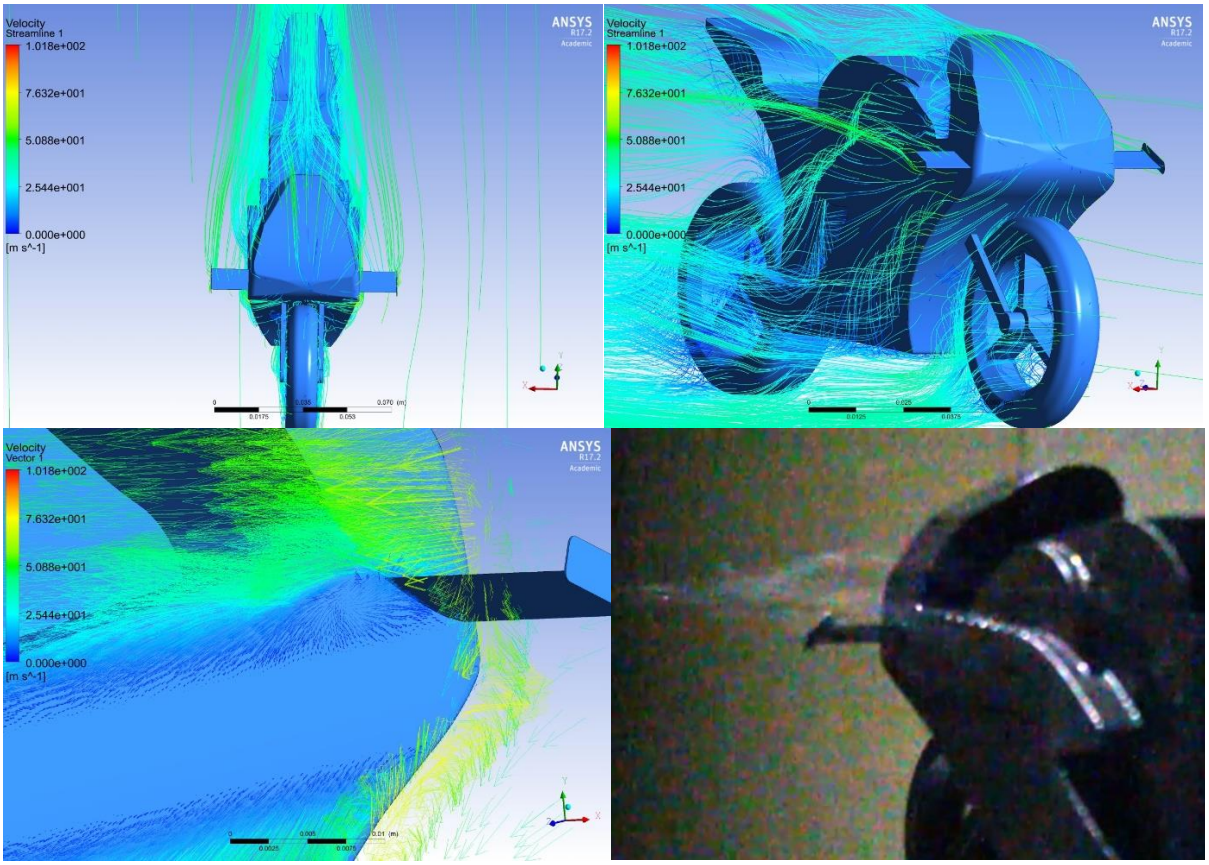

Figure 24. Validation of CFD Results: Wingtip Vortices and Flow Deflection due to the Airfoil.

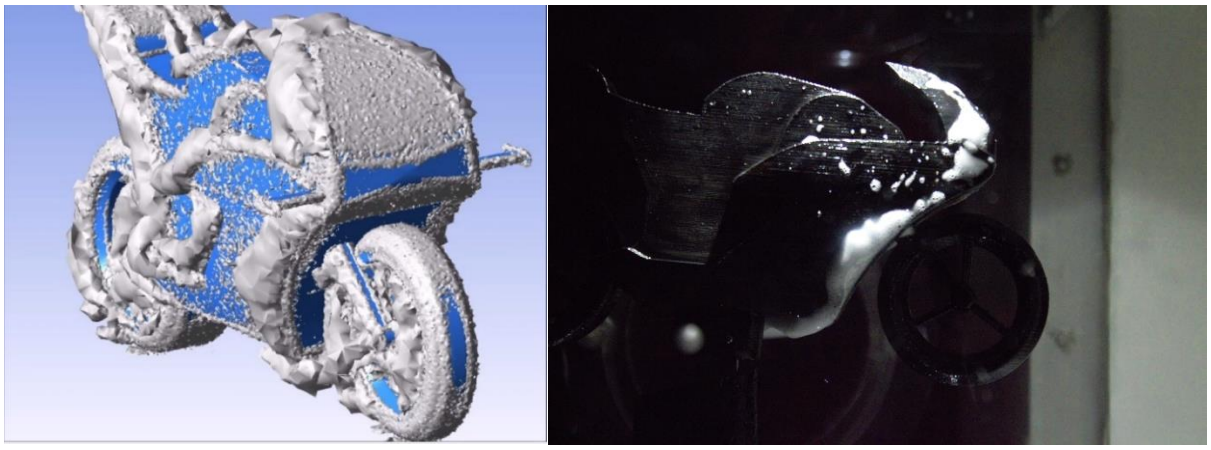

Figure 25. Validation of CFD Results: Vortex Core Region Formation.

Thus, the comparisons of the key aerodynamic flows have a strong correlation. This provides the evidence that indeed, the concept has been validated. This completes the analysis of the project's results. The final chapter provides insights into how the results have provided a room for improvement in the field of motorcycle aerodynamics, efficiency, and safety. The final chapter also deals with the recommendations for future studies that can be performed to advance research into this field.

www.manaraa.com

CHAPTER 8 – CONCLUSIONS AND FUTURE SCOPE

The chapter is divided into two main sections i.e. the Conclusions and the Future Scope.

RESULTS AND CONCLUSIONS

The results of the study were validated. The values found through the CFD are utilized to draw conclusions. The primary conclusions are to assess the improvements that the concept is capable of providing in terms of aerodynamics, efficiency, and safety. The comparisons were performed separately to evaluate the improvements in downforce when the attack angle of the wing was at 0 and 10 degrees as follows. Any improvements in the lift are most important in this case. Any improvement in drag is appreciated as well.

Model Name	Lift	Improvement	Drag	Improvement
Non-Wing	0.04682	< 1%	0.25626	6%
0 Degrees	0.04659		0.24133	

Table 6. Improvements in Downforce - Non-Wing vs. 0 Degree Wing Model.

Model Name	Lift	Improvement	Drag	Improvement
Non-Wing	0.04682	**+23%**	0.25626	-4%
10 Degrees	-0.01178		0.26513	

Table 7. Improvements in Downforce - Non-Wing vs. 10 Degree Wing Model.

In the case of the 90-degree wing model, the lift was not evaluated as the concept was only meant to assess the amount of aerodynamic braking the wing was capable of providing. Thus, in contrast to the tables above, any increase in drag yields a positive effect here and hence is termed with a positive sign in front of the improvement percentage figures.

Model Name	Lift	Improvement	Drag	Improvement
Non-Wing	0.04682	N/A	0.25626	**+15%**
90 Degrees	N/A		0.29496	

Table 8. Improvements in Drag Force - Non-Wing vs. 90 Degree Wing Model.

www.manaraa.com

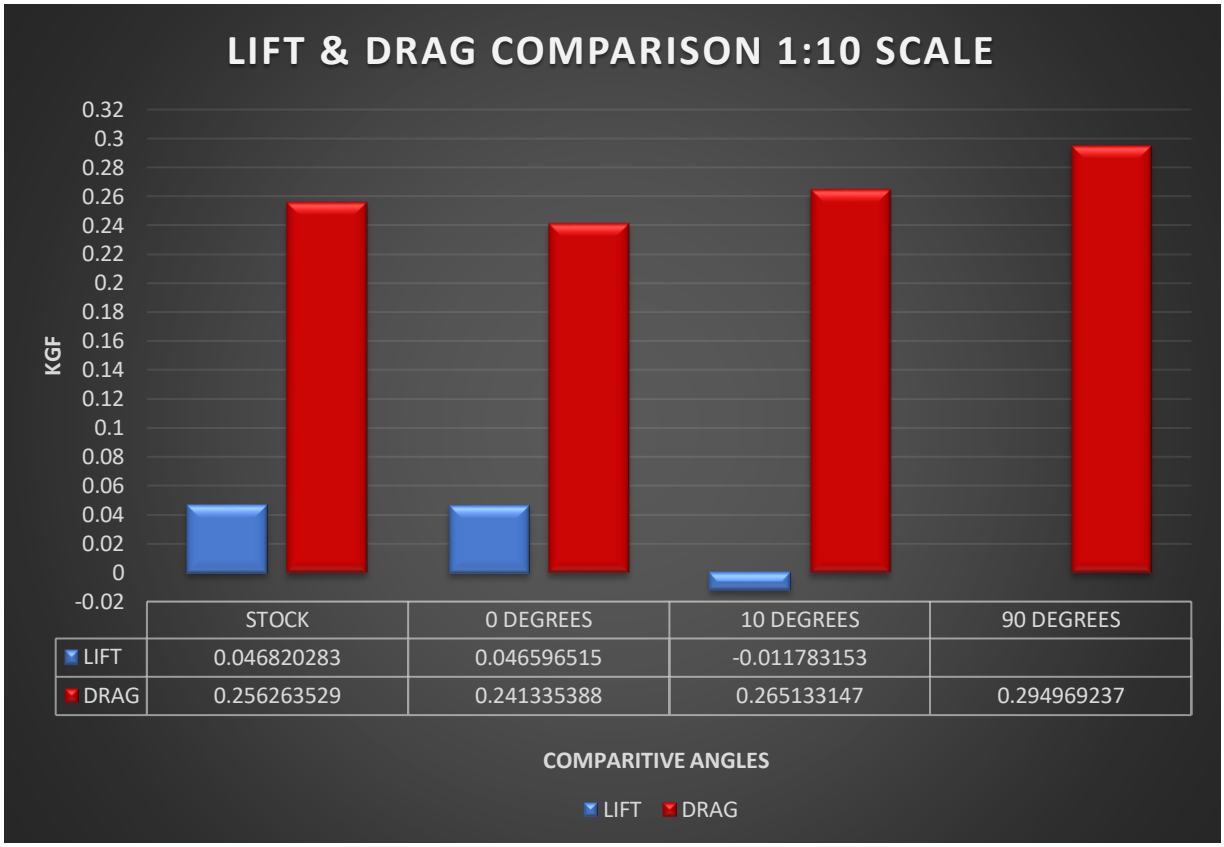

Figure 26. Graphical Representation of Lift vs. Dragforce figures.

Contextual conclusions for the modifications compared to non-wing models were:

- The 0-degree model showed a small improvement in downforce & drag.
- The 10-degree model showed massive improvements in downforce.
- The 90-degree model showed tremendous improvements in drag (braking) force.

FUTURE SCOPE AND RECOMMENDATIONS

These are a few recommendations from the author for the future research on this topic.

- A study on the effects of the airfoils over the full range of attack angles.
- A study on the effects of the airfoil interference during cornering.
- A study on the effects of crashing with deployed airfoils requiring Non-Linear Explicit Dynamics simulations.
- A study on the behavior of tires and tire loads under aerodynamic forces being produced by the airfoils at various attack angles.

The author would like to thank everyone who has read this report and would be willing to assist in any research related to this topic or this field of engineering. Thank you!

www.manaraa.com

APPENDIX

WIND TUNNEL APPARATUS SETUP

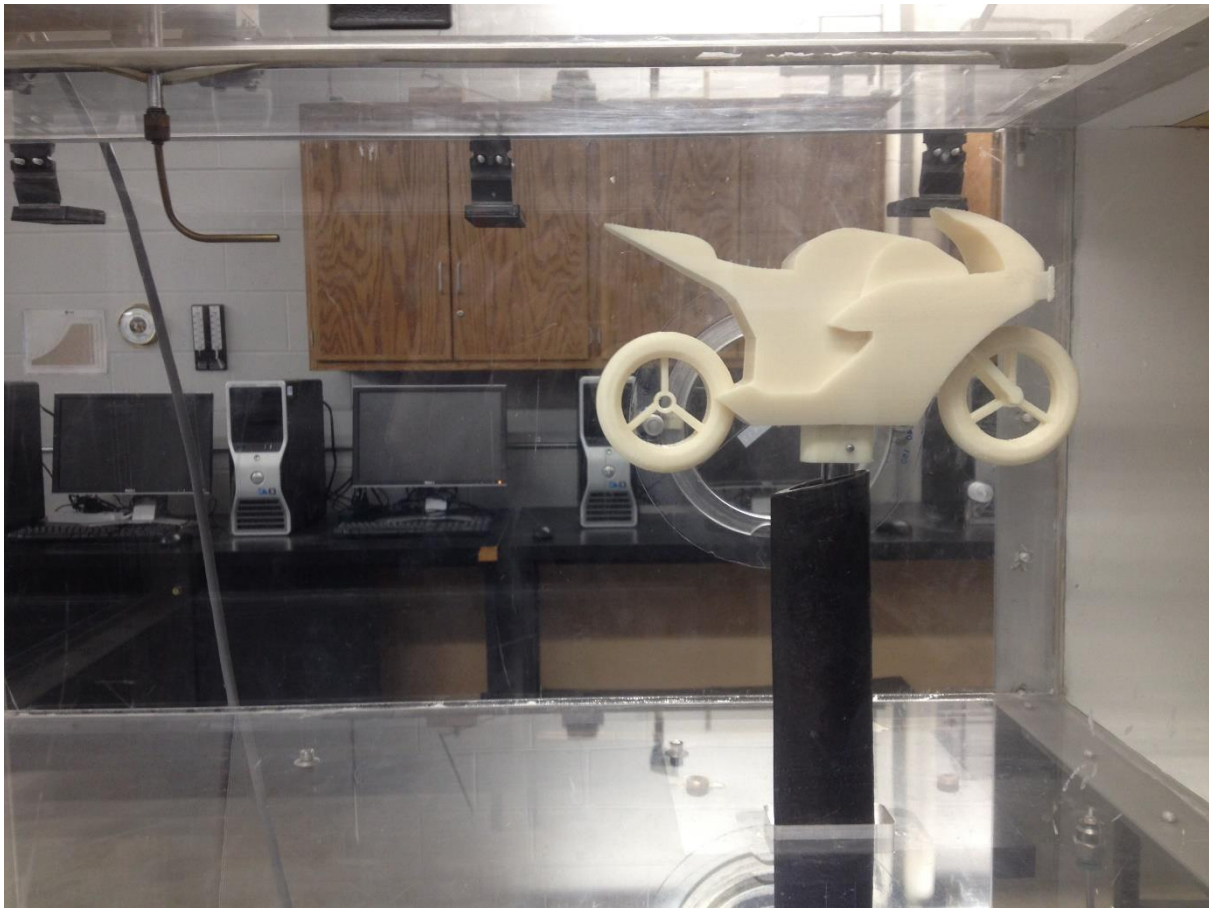

Figure 27. The Strut, Mounting Fixture in the Wind Tunnel.

www.manaraa.com

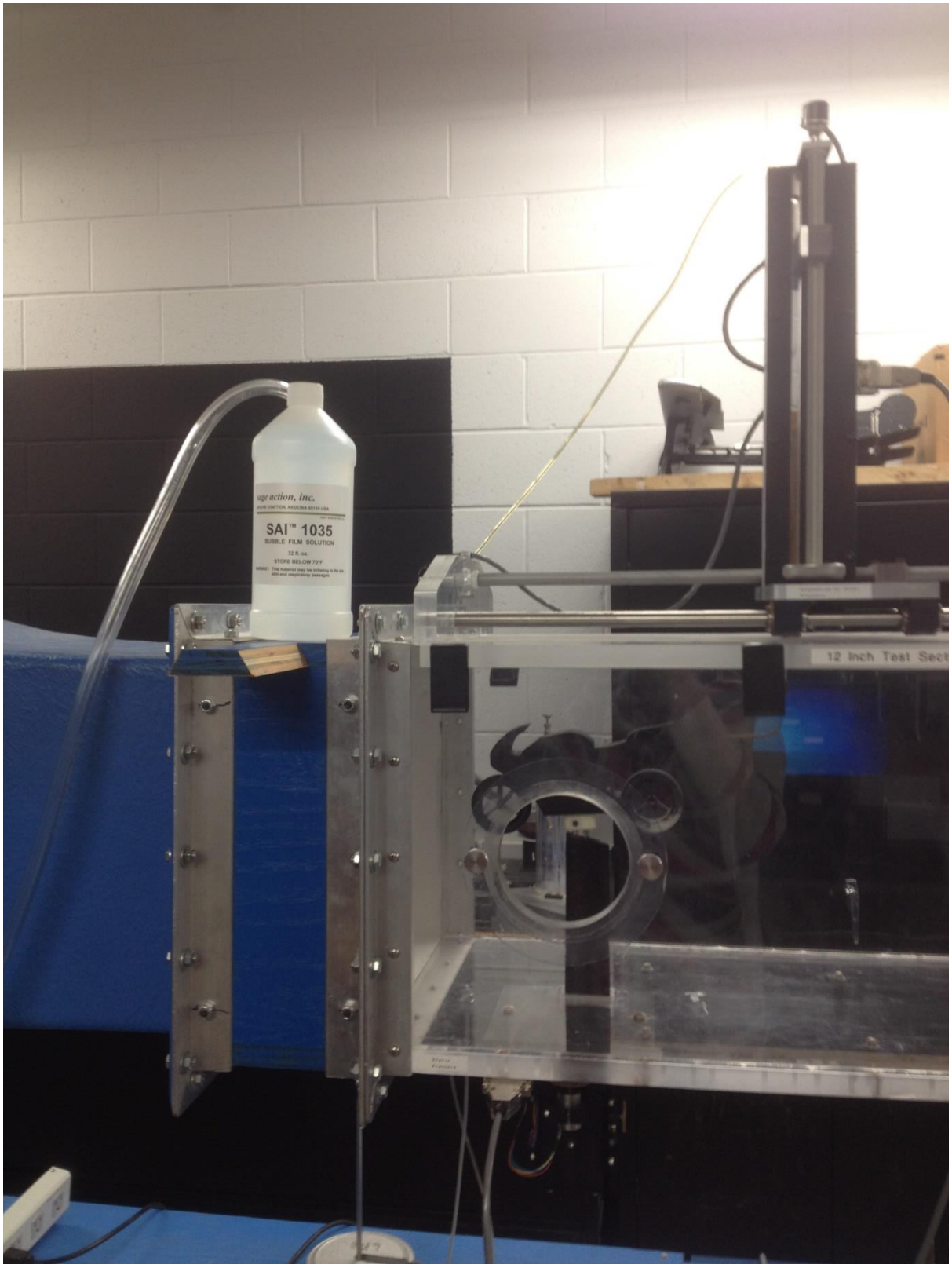

Figure 28. SAI Bubble Solution Equipment, Strut, Mounting Fixture, Prototype and Pitot Tube Assembly.

www.manaraa.com

ELD WIND TUNNEL ELECTRONIC DISPLAY MACHINE OUTPUT

Non-Wing Prototype Force Values:

Figure 29. Non-Wing Prototype Gauge Indication at Zero Wind Speed.

www.manaraa.com

Figure 30. Non-Wing Prototype Gauge Indication at 44.7m/s i.e. Test Wind Speed.

www.manaraa.com

0 Degree Wing Prototype Force Values:

Figure 31. 0 Degree Wing Prototype Gauge Indication at Zero Wind Speed.

www.manaraa.com

10 Degree Wing Prototype Force Values:

Figure 32. 10 Degree Wing Prototype Gauge Indication at Zero Wind Speed.

www.manaraa.com

Figure 33. 10 Degree Wing Prototype Gauge Indication at 44.7m/s i.e. Test Wind Speed.

www.manaraa.com

90 Degree Wing Prototype Force Values:

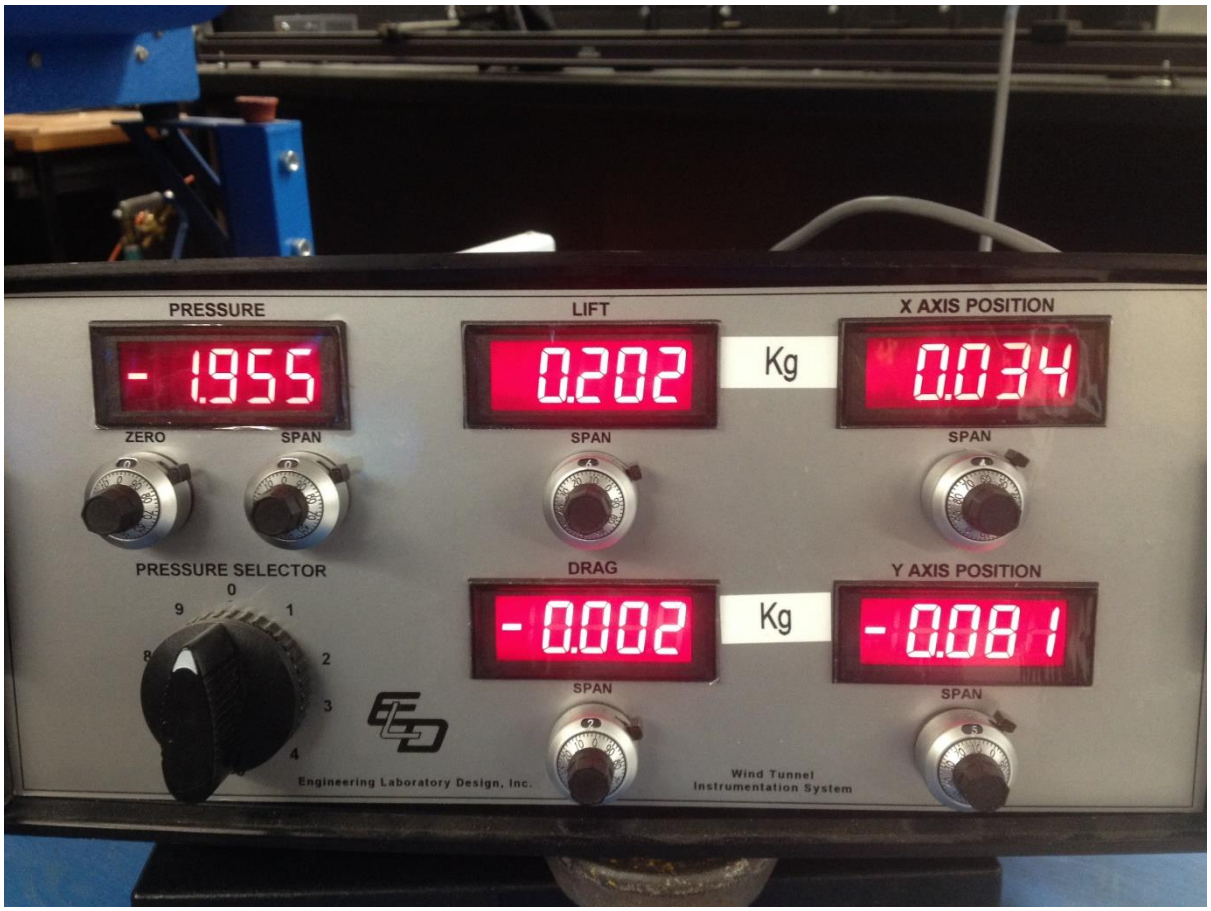

Figure 34. 90 Degree Wing Prototype Gauge Indication at Zero Wind Speed.

www.manaraa.com

Figure 35. 90 Degree Wing Prototype Gauge Indication at 44.7m/s i.e. Test Wind Speed.

www.manaraa.com

BIBLIOGRAPHY

Berman, B. (2011). *3-D printing: The New Industrial Revolution.* Bloomington, Indiana: Kelley School of Business, Indiana University.

CAE Users. (n.d.). Retrieved from The IGES, DXF and STEP Exchange Formats IGES IGES - CAE Users: http://homepages.cae.wisc.edu/~me232/info/dxf_iges_step.pdf

Chakrabarty, A., Mannan, S., & Cagin, T. (2015). *Multiscale Modeling for Process Safety Applications.* Butterworth-Heinemann.

Chung, T. (2002). *Computational Fluid Dynamics.* Press Syndicate of the University of Cambridge.

Davidson, L. (2016). *An Introduction to Turbulence Models.* Goteborg, Sweden.: Chalmers University of Technology.

Edinformatics - What are Fluids? (n.d.). Retrieved from Edinformatics: http://www.edinformatics.com/math_science/what_are_fluids.htm

Engineering Laboratory Design, I. (2007). Wind Tunnel Instrumentation. Lake City, Minnesota, USA.

Fluent Theory Guide. (n.d.). Retrieved from Sharcnet: https://www.sharcnet.ca/Software/Ansys/17.2/en-us/help/flu_th/flu_th.html

Goudar, N., & Lalwani, B. J. (2014). *Aerodynamic Braking for High-Speed Motorcycles.* SAE International.

Hall, N. (2015, May 5). *Glenn Research Center - National Aeronautics and Space Administration - What is Lift?* Retrieved from Glenn Research Center - National Aeronautics and Space Administration: https://www.grc.nasa.gov/WWW/K-12/airplane/lift1.html

J.D. Anderson, J. (2009). Governing Equations of Fluid Dynamics. In J. W. (ed.), *J.F. Wendt (ed.), Computational Fluid Dynamics, 3rd ed.,.*

J.H.Ferziger, M. (2002). *Computational Methods for Fluid Dynamics 3rd Edition.* New York.

Kankanamge, S. A. (2015). *Air Flow and Rain Water Penetration Analysis on Generator Enclosures Using CFD Simulations.* Mankato: Cornerstone: A Collection of Scholarly and Creative Works for Minnesota State University, Mankato.

Kleinstreuer, C. (2010). *Modern Fluid Dynamics - Basic Theory and Selected Applications in Macro- and Micro-Fluidics.* Springer Netherlands.

Lee, H.-H. (2014). *Finite Element Simulations with ANSYS Workbench 15: Theory, Applications, Case Studies.* Mission, Kansas: Stephen Schroff, SDC Publications.

Maria, A. (1997). *Introduction to Modelling and Simulation.* Binghamton, NY USA: State University of New York at Binghamton, Department of Systems Science and Industrial Engineering. Retrieved from http://imap.acqnotes.com/Attachments/White%20Paper%20Introduction%20to%20Modeling%20and%20Simulation%20by%20Anu%20Maria.pdf

MCN Bikes For Sale. (n.d.). Retrieved from Motorcycle News.Com: http://www.motorcyclenews.com/bike-reviews/honda/cbr1000rr-fireblade/2004/

www.manaraa.com

Menter, F. R., Langtry, R. B., Likki, S. R., Suzen, Y. B., Huang, P. G., & Völker, S. (2006). *A Correlation-Based Transition Model Using Local Variables Part I: Model Formulation.*

National Training and Simulation Association . (2011). *A Primer on Modeling and Simulation.* Retrieved from http://www.trainingsystems.org/NTSA_Primer_on_Modeling_and_Simulation.pdf

Nitin, S. G., & Lee, G. (2008). Introduction to Meshing. In S. G. Nitin, S. Sanjay, & V. Sanjeev, *Practical Finite Element Analysis.* Altair University.

Park, K., Hong, C. H., Kim, K. S., & Lee, J. (2008). Effect of Endplate Shape on Performance and Stability of Wings-in Ground (WIG) Craft. *International Journal of Mechanical, Aerospace, Industrial, Mechatronic and Manufacturing Engineering Vol:2, No:11,*, 1237.

Romander, E., Norman, T. R., & Chang, I.-C. (2011). *Correlating CFD Simulation With Wind Tunnel Test for the Full-Scale UH-60A Airloads Rotor.* Moffett Field, California: NASA Ames Research Center.

Sage Action, I. (2002). SAI Bubble Generator Model 5 Console - Description and Operating Instructions. Ithaca, New York, USA.

Sedlak, V. (2012). *Motorcycle Cornering Improvement: An Aerodynamical Approach based on Flow Interference.* Stockholm: Royal Institute of Technology.

Sokolowski, J. A., & Banks, C. M. (2010). *Modeling and Simulation Fundamentals: Theoretical Underpinnings and Practical Domains.* John Wiley & Sons.

Suhas, V. P. (1980). *Numerical Heat Transfer and Fluid Flow.* Minneapolis: Taylor & Francis.

Sun, D.-W. (2007). *Computational Fluid Dynamics in Food Processing.* Boca Raton; London; New York: CRC Press.

T.M.V Engineering Blog. (n.d.). Retrieved from Welcome to T.M.V Engineering Blog: http://timmsvillee.blogspot.com/2014/08/available-courses-who-should-attend.html

Thisse, E. (2004). *Influence Of End-Plates On Tip Vortices In Ground Effect For A 2004 Formula One Front Wing.* Cranfield, England: Cranfield University.

Tu, J., & Guan Heng, Y. (2007). *Computational Fluid Dynamics : A Practical Approach.* Burlington, MA: Butterworth-Heinemann.

UIUC Airfoil Coordinates Database. (n.d.). *Airfoil Tools*. Retrieved from airofoiltools.com: http://airfoiltools.com/airfoil/details?airfoil=naca6412-il

Varela-Boydo, C. A., & Castro-Gómez, L. L. (2015). Numerical and Experimental Study of a Scale Bus Model in Wind Tunnel. *Journal of Traffic and Transportation Engineering 3*, 301-308.

Versteeg, H., & Malalasekara, W. (1995). *Computational Fluid Dynamics: The Finite Volume Method.* Essex, England: Longman Scientific & Technical.

Wendt, J. F., Anderson, J. D., & Von Karman Institute. (2008). *Computational fluid dynamics: An Introduction.* Berlin; London: Springer.

Zikanov, O. (2010). *Essential Computational Fluid Dynamics.* Hoboken, N.J: Wiley.

www.manaraa.com